ISSN 2718-322X (Online)

Engineering Power

BULLETIN OF THE CROATIAN ACADEMY OF ENGINEERING Vol. 20(1) 2025

EDITOR-IN-CHIEF'S WORD

Dear Readers,

It is my pleasure to introduce a new edition of Engineering Power, which addresses the complex and technically demanding field of explosives — an area that lies at the intersection of fundamental science, engineering practice, safety considerations, and environmental responsibility.

The contributions in this issue exemplify how modern computational methods and meticulous experimental work complement one another: numerical modelling helps narrow down viable formulations and scenarios, while targeted experiments validate these models and uncover practical limitations. This synergy is essential for developing solutions that meet stringent safety standards while delivering the performance demanded by industry and large-scale infrastructure projects.

The work presented here clearly demonstrates the Academy's growing role in tackling challenges that are both technically complex and socially significant.

Editor-in-Chief
Vedran Mornar, President of the Croatian Academy of Engineering

EDITOR'S WORD

Dear Readers,

The first issue of Engineering Power in 2025 was edited by Prof. Mario Dobrilović, PhD, from the University of Zagreb, Faculty of Mining, Geology and Petroleum Engineering. The articles in this issue are dedicated to the topic of explosives and cover the prediction of explosives performance, new secondary explosives and oxidising agents, and modelling of soil density zones in the vicinity of an explosive charge. There is also an overview of the 55th Ordinary Annual Assembly of the Croatian Academy of Engineering and the 3rd Mini Scientific and Professional Conference which was held as part of the Assembly. I hope you enjoy reading this issue.

Editor
Bruno Zelić, Vice- President of the Croatian Academy of Engineering

FOREWORD

Dear Readers,

Explosives are energetic materials that undergo extremely rapid chemical decomposition, releasing large amounts of energy. Their properties range from highly brisant military explosives to insensitive military explosives and safe civil emulsion explosives. Beyond military uses, probably more significant application is civilian: explosives enable the mining of large quantities of coal and metallic and non-metallic ores and make possible the fragmentation and movement of vast volumes of material required by major infrastructure, energy and transportation projects.

The foundations of detonation theory were established relatively recently — principally during the 1940s and throughout World War II. The so-called "ideal" military explosives are chemically pure, often monomolecular compounds discovered near the end of the nineteenth century and deployed extensively during the two world wars. In contrast, commercial (civil) explosives were developed primarily after World War II to meet growing demands for raw materials and economic development. Today's civil explosives are predominantly heterogeneous mixtures whose individual components are not explosive in themselves; their detonation behaviour does not fully conform to classical ideal detonation theory, which makes their modelling a still challenging task.

Explosives remain energetic materials with modest heat content per unit mass but extraordinarily fast detonation processes that concentrate energy over microsecond timescales, producing pronounced destructive effects. Advances in computational power now permit thermochemical and hydrodynamic (hydrocode) modelling of new formulations — both monomolecular and mixtures — to assess their likely performance and practical usefulness prior extensive experimental testing. For example, Professor Klapotke's successful synthetic approaches have been documented along with the detonative property modelling carried out using a domestic thermochemical code developed by Professor Sućeska.

Although the primary use of civil explosives is rock fragmentation, their application in soils is also important. Modelling studies that compare numerical predictions with experimental measurements in clayey soils — using non-ideal commercial explosives — help to validate models and improve predictive capability for ground-coupled blasting scenarios.

Where is explosive technology heading? Military research continues to seek compounds that detonate faster and generate higher pressures and temperatures to maximize destructive effect while improving safety and insensitivity to accidental initiation. Civil formulations, meanwhile, are being driven toward safer, more environmentally acceptable compositions that still deliver required performance at acceptable cost. Explosives will remain indispensable in the future; the hope is that their future role will shift from military to more civilian applications, including advanced sectors such as space technology.

Guest Editor
Mario Dobrilović, University of Zagreb, Faculty of Mining, Geology and Petroleum Engineering

CONTENT

Muhamed Sućeska[1]

Accuracy of prediction of explosives performance using an analytic equation of state for EXP-6 potential fluid

University of Zagreb, Faculty of Mining, Geology, and Petroleum Engineering, Pierottijeva 6, 10000 Zagreb

Abstract

Explosive materials undergo rapid chemical reactions, followed by the release of (mostly) gaseous products and heat energy. The performance of an explosive is most often quantified in terms of released heat energy, detonation velocity, volume of released gases, and pressure generated. The possibility to accurately predict these parameters is essential for designing more efficient explosives.
In this paper, it is shown that using the analytic equation of state for EXP-6 potential fluid, incorporated into the thermochemical code EXPLO5, the detonation velocities and pressures of ideal explosives can be predicted with a maximum error comparable to the measurement errors.

Keywords: *explosives, detonation, thermochemical calculation, EXP-6 EOS, EXPLO5 code*

1. Introduction

The explosives community is constantly searching for more efficient and safer explosives for military and commercial applications. Traditional methods of developing new explosives and explosive formulations typically require extensive experimental work involving material synthesis and testing, which is time-consuming, resource-intensive, and associated with considerable safety risk [1,2].

With the development of computers and efficient numerical methods, theoretical prediction of explosive performance plays an increasingly important role and is now an indispensable part of the development process. Numerical modeling has revolutionized the way researchers approach the development of new explosives, enabling a significant reduction in research time, resources, and costs, compared to the traditional approach. Today, several methodologies are used to theoretically predict explosive properties and performance. Thanks to them, researchers can explore a large number of potential explosives and predict their properties and performance even before they are synthesized. In this way, it is possible to identify promising explosives much more quickly and focus on them in further laboratory testing.

For example, computational thermodynamics (quantum chemistry and molecular dynamics) can be used to calculate the thermodynamic properties of potential explosive molecules and to provide detailed insights into their molecular structure and behavior. Such calculation can provide the enthalpy of formation [3,4] and density [5], which are input parameters for thermochemical codes used for the calculation of detonation parameters.

Hydrodynamic codes (such as LS-Dyna, Autodyn, etc.) can be used to model the fluid hydrodynamics associated with the detonation of explosives. It includes modeling the shockwave propagation, initiation and propagation of detonation, expansion of gaseous products, and the response of surrounding materials to the explosion [6,7]. This calculation provides information about the effects of explosives under specified conditions, which facilitates the design of more efficient systems for military and industrial applications.

Thermochemical equilibrium codes solve thermodynamic equations between detonation products to find the chemical equilibrium at specified volume, pressure, and temperature [8]. When coupled with the Chapman-Jouguet (C-J) detonation theory, they can predict detonation parameters such as detonation velocity, detonation pressure, heat, composition and concentration of detonation products, etc. [8, 9]. The first thermochemical codes appeared about 70 years ago (the RUBY code, Lawrence Radiation Laboratory, USA), and the BKW code (Los Alamos Scientific Laboratory, USA). In the 1960's, Stanford Research Institute developed the TIGER code. In 1994, Lawrence Livermore Laboratory converted the TIGER code to the CHEETAH code [10]. At the beginning of the 21st century, a few more codes appeared: TDS [11], EXPLO5 [9], CARTE [12] and others.

The mentioned codes are based on the Chapman-Jouguet detonation theory of detonation [13,14], with CHEETAH and EXPLO5 having also a built-in Wood-Kirkwood detonation model [15] that allows the calculation of detonation parameters for non-ideal explosives. The key difference between the codes is in the equations of state they use to describe the state of gaseous and condensed

products under conditions of extremely high pressure and temperature.

In addition to thermochemical codes, simpler empirical equations are often used to predict certain detonation parameters. These equations correlate various physical and chemical properties of explosives with their performance parameters such as detonation velocity, pressure, and energy output [1, 2, 16, 17, 18]. An excellent review of empirical equations and their accuracy is given in the paper by Muravyev et al. [1]

Machine learning and artificial intelligence have recently become increasingly relevant in the theoretical prediction of explosive performance [19, 20]. These emerging fields have the potential to significantly contribute to the improvement of the accuracy of performance prediction of potential explosives.

Although thermochemical equilibrium codes have been in use for several decades and are an indispensable tool in predicting the output of detonation, there are still challenges related to improving the accuracy of prediction. This paper deals with the accuracy of the prediction of key detonation parameters using an analytic equation of state for EXP-6 potential fluid, incorporated into thermochemical code EXPLO5, with an emphasis on the influence of some input parameters on the accuracy.

2. Description of detonation model

Upon initiation explosives undergo a series of rapid chemical reactions, producing (mainly) gaseous products and thermal energy. Explosive reactions are self-sustaining and propagate layer-by-layer through the explosives. Depending on the way of initiation and characteristics of the explosive, they may propagate at subsonic (e.g., combustion and deflagration) or supersonic velocities (detonation). Unlike combustion, detonation produces a shock wave that travels at a speed approaching 10 km/s, reaching 50 GPa pressure, and 6000 K temperature in nanoseconds [8]. Due to such extreme conditions, the energy transport from reacted to the unreacted layer of explosive by heat conduction, viscosity, and radiation is negligibly small compared to energy transport by motion (shock wave). Under such pressure the strength of any explosive material is negligible, and it responds hydrodynamically. The detonation process may be described by the Chapman-Jouguet (C-J) and Zeldovich-von Neumann-Doring (ZND) hydrodynamic detonation theories based on the conservation of mass, momentum, and energy across a jump-wise transition from unreacted to a reacted state of explosive [13,14].

The transformation of CHNO explosives into detonation products may be described by the following generalized formula:

$$C_cH_hN_nO_o \rightarrow n_1H_2O + n_2H_2 + n_3O_2 + n_4CO_2 + n_5CO + n_6CH_4 + n_7NH_3 + n_8N_2 + n_9NO + n_{10}C + \ldots$$

where n_1 - n_N are the mol amount of individual products. The transformation occurs very fast (on a nanosecond or microsecond scale, depending on the properties of the explosive). The C-J detonation model, incorporated in EXPLO5 code, assumes explosives transform into products instantly, so kinetics of reactions does not play a role. The heat generated in the reactions heats the detonation products to several thousand degrees, resulting in the generation of pressure of several tenths of GPa. In conditions of such high temperature and pressure, the detonation products represent a reactive system in which rapid reactions between individual products take place. As a result, the state of thermochemical equilibrium establishes very rapidly, resulting in no change in the concentration of products over time. The equilibrium concentration (i.e., mole numbers) of individual detonation products can be calculated by minimising the Gibbs free energy, preserving simultaneously the mass balance principle [21,22]. For a mixture of detonation products consisting of N different chemical species being in M different phase states, Gibbs free energy (G) is a function of temperature, pressure, and mole number of each product in each phase (n_i^k) [21]:

$$G = \sum_{k=1}^{M} \sum_{i=1}^{N} n_i^k \mu_i^k \quad (1)$$

where n_i^k is the number of moles of product i in phase k, and μ_i^k is the chemical potential of product i in phase k

To determine the equilibrium composition of detonation products by minimising the Gibbs free energy, EXPLO5 uses a method developed by White et al. [22] and adapted for computer application by Mader [13]. The method involves forming and solving a system of nonlinear equations, derived from the established thermodynamic relationships, in which the concentrations of individual products (n_i^k) are unknown. The calculation gives the product concentration and the thermodynamic functions at a specified volume (or pressure) and temperature. By combining this calculation with the C-J detonation theory, detonation parameters such as detonation velocity, pressure, heat, temperature, etc., can be derived.

EXPLO5 determines the C-J point as a point on the shock adiabat of detonation products at which the detonation velocity, calculated by Eq. 2, has its minimum value [13]:

$$D = V_0 \sqrt{\frac{p - p_0}{V_0 - V}} \quad (2)$$

where D is the detonation velocity, p_0 and V_0 are the initial pressure and volume of the explosive, p and V are the pressure and volume of products on the shock adiabat of products. To find the minimum of D, i.e., the C-J point, a minimisation algorithm is employed. Once the C-J point is determined, the detonation parameters are derived using the relationships that follow from the C-J theory.

An integral part of the EXPLO5 code is an extensive database of explosives and ingredients of explosive mixtures (containing explosive formulas, densities, and enthalpies of formation), and a database of products containing three sets of information: a) formula, enthalpy of formation, and density, b) polynomial constants describing the dependence of standard thermodynamic functions on temperature, and c) constants in the equations of state of gaseous and condensed detonation products.

Equations of state of gaseous and condensed products

The C-J detonation model is supplemented by equations of state (EOS) capable of describing accurately the thermodynamic behaviour of condensed and gaseous products in a very broad range of pressures and temperatures. Until about 20 years ago, all thermochemical codes used semi-empirical EOS (most often the Becker-Kistiakowsky-Wilson EOS, BKW), while more recently sophisticated theoretically based fluid EOS have been increasingly used [11,12,23]. Such an equation, named EXP-6, is incorporated in the EXPLO5 code [9, 24]. It is based on statistical mechanical theory and the Buckingham α-exponential-6 (EXP-6) model to describe the interaction energy between the product [8]:

$$u(r) = \frac{\varepsilon}{\alpha - 6}\left[6e^{\alpha(1-r/r_m)} - \alpha\left(\frac{r_m}{r}\right)^6\right] \quad \text{for } r > r_c \qquad (3)$$

$$u(r) = \infty \quad \text{for } r \le r_c$$

where $u(r)$ is the central pair potential; ε is the depth of attractive well between particles, r is separation distance, r_m is the position of the potential well minimum, α is the stiffness of the repulsive potential; first term in square brackets describes repulsive forces, second term attractive forces.

Direct implementation of Eq.3 in a thermochemical code would result in an unacceptably long calculation time, regardless of what statistical mechanical theory is applied. This drawback was successfully solved by Byers Brown [25] who proposed a method based on the analytical representation of the excess Helmholtz free energy (A^{ex}) in terms of transformed thermodynamic variables. According to the author, the excess Helmholtz free energy function ($F=A^{ex}/Nk_BT$) for the one-fluid mixture model (which assumes a mixture of products is a hypothetical one-component fluid with an effective EXP-6 potential) can be expressed as a function of three reduced variables; α, T*, and ρ* [25]:

$$F(\alpha, T^*, \rho^*) = \frac{A^{ex}(T,V,N;\, r_m,\varepsilon,\alpha)}{Nk_BT} \qquad (4)$$

where F is the excess free energy function, T* and ρ* are dimensionless temperature and density ($T^* = k_BT/\varepsilon$, $\rho^* = Nr_m^3/V$), respectively; k_B is the Boltzmann constant, N is the number of particles, and V is volume.

For the practical application of Eq. 4, Byers Brown proposed a three-variable (α,T^*,ρ^*) analytical representation of the excess free energy function $F(\alpha,T^*,\rho^*)$ using the Chebyshev polynomials. The author determined polynomial coefficients using $F(\alpha,T^*,\rho^*)$ values generated by applying the Weeks-Chandler-Anderson/Ree (WCA/Ree) hard-sphere perturbation theory [25]. Once $F(\alpha,T^*,\rho^*)$ is known, the excess Helmholtz free energy can be derived ($A^{ex}=F\cdot Nk_BT$). All other thermodynamic quantities can then be derived from A^{ex} [25, 26]:

$$p = -\left(\frac{\partial A(V,T)}{\partial V}\right)_T$$

$$S(V,T) = -\left(\frac{\partial A(V,T)}{\partial T}\right)_V \qquad (5)$$

$$\mu_i = \left(\frac{\partial A(V,T)}{\partial n_i}\right)_{V,T,\{n\}}$$

$$E(V,T) = A(V,T) + T \cdot S(V,T)$$

Eq. 4 represents a trivariate analytical representation of the thermodynamic equation of state based on EXP-6 potential [25]. EXPLO5 uses multinomial coefficients of order 4x4x4 (64 polynomial coefficients) to describe the $F(\alpha,T^*,\rho^*)$ function in α, T^*, ρ*domains of interest in detonation physics [9,24]. In addition to the multinomial coefficients, the interaction potential parameters (r_m, ε, α) for each gas phase detonation product must be known. The values of potential parameters for main detonation products are given in Table 1.

Table 1. The like-pair EXP-6 potential parameters for main detonation products

Product	$r_{m,ii}$ (Å)	ε_{ii}/k_B (K)	α_{ii}	λ_{ii}	Ref.
H_2O	3.25	188.0	13.3	496	[27]
H_2	3.49	30.4	11.2	0	[2]
O_2	3.83	121.2	13.6	0	[23]
CO_2	4.22	230.2	13.8	0	[29]
CO	4.16	105.5	13.2	0	[23]
N_2	4.13	101.0	13.1	0	(24)
CH_4	4.30	137.8	12.3	0	[23]
CH_2O_2	4.62	150.0	13.0	0	(24)
NH_3	3.95	96.7	12.9	117	[27]
NO_2	4.27	338.0	13.6	0	[23]
NO	3.71	151.9	13.1	0	[23]

For polar molecules, such are H_2O, NH_3, etc., EXPLO5 uses temperature-dependent well depth, as suggested by Ree [26]:

$$\varepsilon_{ii}(T) = \varepsilon_{0,ii}\left(1 + \frac{\lambda_{ii}}{T}\right) \qquad (6)$$

where λ_{ii} is constant (for non-polar molecules $\lambda_{ii} = 0$).

Under high pressures condensed detonation products are compressible and their compressibility is described by Murnaghan EOS [30]:

$$V = V_0[n\kappa P + \exp\{-\alpha_e(T - T_0\}]^{-\frac{1}{n}} \qquad (7)$$

where: V_0 is the molar volume when p=0 and T=T_0, T_0 is the temperature of the reference isotherm (298.15 K), κ is the inverse of the isothermal bulk modulus, α_e is the volumetric coefficient of thermal expansion, n is the constant.

Condensed carbon represents an important detonation product for some explosives. It is assumed in this paper that condensed carbon forms two solid phases (diamond and graphite) and two liquid phases (diamond-like and graphite-like liquid phases) [31], where the concentration of individual phases is determined by the phase equilibria at the given p, V, T conditions. The Murnaghan parameters for condensed carbon, used in this study, are given in Table 2.

Table 2. Parameters in Murnaghan EOS of condensed carbon

Phase	ΔH_f^o (kJ/mol)	V_0 (cm³/mol)	α_e, (m/mK)	κ_0, (1/bar)	n
Graphite	28.2	5.286	2.32E-05	2.32E-06	7.1
Diamond	21.1	3.64	2.43E-06	2.30E-07	2.4
Graphite-like liquid	81	6.00	2.32E-05	2.32E-06	7.1
Diamond-like liquide	125	3.95	2.43E-06	2.96E-07	2.4

Legend: Values of ΔH_f^o taken from Viktorov et al. [32], V_0 taken from Fried and Howard [31], and values of α_e, κ_0, and n taken from Suceska [9].

3. Experiment and discussion

To estimate the accuracy of prediction of detonation velocity (D) and detonation pressure (p_{CJ}) using the EXP-6 equation of state, a set of explosives for which reliable experimentally determined D and p_{CJ} exist was used. The set consists of several standard and well-characterised individual high explosives (RDX, HMX, TNT, PETN, NG, NM, TNM, Tetryl, etc.), four mixture-type of explosives (RX-23-AA, RX-23-BB, RX-23-CC, ANFO), and three explosives that exhibit non-ideal behaviour (ANFO, TATB, NQ). A total of 48 explosives of different compositions (CHNO, CNO, HNO, and NO) and densities (from 0.25 to 1.97 g/cm³) were analyzed (Table 3).

Model derivation

Input parameters for thermochemical calculation include parameters of explosives (formula, density, and enthalpy of formation) and parameters of detonation products (EOS of gaseous and condensed products and thermodynamic functions of the state as a function of temperature). The detonation parameters of studied explosives are calculated for the initial densities of explosives (ρ_0) at which the detonation velocities and pressures are measured. The enthalpies of formations are taken from the EXPLO5 database [9]. The EXP-6 potential parameters (r_m, ε/k_B, α) for the main detonation products used in the calculations are listed in Table 1, and the parameters in Murnaghan EOS of condensed carbon are given in Table 2. The thermodynamic functions of detonation products in their standard state are calculated from the enthalpy, where the dependence of enthalpy on temperature is expressed by a fourth-degree polynomial. The dependence of thermodynamic functions on temperature is taken from JANAF thermochemical tables [33].

Validation of model against experimental data

The detonation velocity is a detonation parameter that can be measured more accurately than other detonation parameters, with an accuracy of ±1 m/s [1]. However, some factors (such as variation in charge density, charge diameter, length, way of initiation, etc.) can significantly affect the measured value, which results in a variation of the experimentally determined velocity by a few percent [13]. The influence of the mentioned factors is much more pronounced in the case of explosives that exhibit non-ideal behavior, that is, a strong dependence of the detonation parameters on the size of the explosive charge. An analysis performed using experimental $D = f(\rho_0)$ data for RDX, HMX, and PETN, published in Hobbs and Baer [34], showed that the maximum difference between the measured detonation velocities and the velocities calculated from the best-fit equation varies from -176 m/s to 218 m/s (MAE=47 m/s, MAPE=0.69%). Chirat and Pittion-Rossillon [35] state that the results of individual authors differ by about 2 % (which corresponds to 60 m/s for D=3000 m/s and 180 m/s for D=9000 m/s).

Experimental determination of the detonation pressure is quite complex and involves different indirect and direct methods [36]. The measuring uncertainty is generally quite large. According to Hobbs and Baer [34] detonation pressures measured by various indirect methods range from 10 to 20 % (which corresponds to 3 to 6 GPa for p_{CJ}=30 GPa), while according to Chirat and Pittion-Rossillon [35] they range from 5 to 10 % (which corresponds to 1.5 to 3 GPa for p_{CJ}=30 GPa). Moreover, Kamlet and Dickinson [37] showed that analysis of the same raw experimental data by different research groups yields detonation pressures that differ up to 3.2 GPa. An analysis conducted in this work using experimental $p_{CJ} = f(\rho_0)$ data for RDX, HMX, and PETN, published in Hobbs and Baer [34], showed that the largest difference between the measured detonation pressures and the pressures calculated from the best-fit equation varies from -13.3 to 19.7 GPa (MAE=5.7 GPa, MAPE=2.7%)

A typical example of the output results of thermochemical calculations, for TNT and HMX, is given in Table 3. The calculated values of detonation velocities and pressures for all studied explosives are given in Table 4.

Table 3. The main calculation results for TNT and ANFO

	Parameter	Explosive name		
		TNT	TNT	HMX
Input parameters	Formula	$C_7H_5N_3O_6$	$C_7H_5N_3O_6$	$C_4H_8N_8O_8$
	ρ_0 (g/cm³)	1.64	1.00	1.90
	ΔH_f^o (kJ/mol)	-59.35	-59.35	74.79
Detonation parameters	Q_d (kJ/kg)	-4610.8	-3864.0	-5683.6
	T_d (K)	3279.2	3196.2	3290.0
	p_{CJ} (GPa)	18.56	6.92732	40.04
	D (m/s)	6793.5	5079.4	9186.2
	M_g (g/kg)	755.1	867.1	966.6
	M_c (g/kg)	244.9	132.9	33.4
	V_0 (dm³/kg)	561.9	728.6	673.9
Detonation products (mol/mol of explosive)	H_2O(g)	1.778923	1.170727	1.689581
	H_2(g)	0.021015	0.334555	0.00223
	N_2(g)	1.459389	1.420841	3.971715
	CO_2(g)	1.346396	0.753262	0.890896
	CO(g)	0.442643	3.088343	0.053333
	CH_2O_2	0.537068	0.105005	2.231501
	NH_3(g)	0.071140	0.096876	0.04740
	C(diamond)	3.696519	0	0.823152
	C(graphite)	0.934918	2.513321	0
	CH_4(g)	0.011813	0.203017	0.000188
	C_2H_4(g)	0.007504	0.11312	0.00008

Legend: ρ_0–initial density, ΔH_f^o– standard enthalpy of formation, Q_d – heat of detonation, T_d – detonation temperature, M_g and M_c – mass of gaseous and condensed products, V_0 – volume of gas at STP

Two important things can be observed from Table 2. First, the composition of detonation products for the same explosive changes with explosive density. For example, 1 mole of TNT having a density of 1.64 g/cm^3 produces 3.696 moles of carbon in the form of diamond and 0.935 moles in the form of graphite, while TNT with a density of 1.0 g/cm^3 produces only carbon in the form of graphite (2.51 moles). Second, detonation parameters (D, p_{CJ}, Q, T, etc.) for the same explosive change with the density of explosives D(at 1.64 g/cm^3)=6793.5 m/s, D(at 1.0 g/cm^3) =5079.4 g/cm^3).

Table 4. Experimental and predicted values of detonation velocities and pressures

Reactant names	Formula	ΔH_f^o (kJ/mol)	ρ_{TMD} (g/cm^3)	ρ_0 (g/cm^3)	$D_{expt.}$ (m/s)	$D_{calc.}$ (m/s)	Dif. (m/s)	p_{CJ_expt} (GPa)	p_{CJ_calc} (GPa)	Dif. (GPa)	Ref.
Octogen (HMX)	$C_4H_8N_8O_8$	74.80	1.905	1.89	9115	9143	27	39.00	39.25	0.25	[34
Octogen (HMX	$C_4H_8N_8O_8$	74.80	1.905	1.60	8040	7981	-59	28.00	26.52	-1.48	[34
Octogen (HMX)	$C_4H_8N_8O_8$	74.80	1.905	1.40	7300	7369	69	21.00	20.60	-0.40	[34
Octogen (HMX)	$C_4H_8N_8O_8$	74.80	1.905	1.20	6560	6700	140	15.70	14.34	-1.36	[34
Octogen (HMX)	$C_4H_8N_8O_8$	74.80	1.905	1.00	5805	5934	128	10.90	9.42	-1.48	[34
Octogen (HMX)	$C_4H_8N_8O_8$	74.80	1.905	0.75	4890	4923	32	6.10	5.13	-0.97	[34
Hexogen (RDX)	$C_3H_6N_6O_6$	70.31	1.806	1.80	8754	8766	11	34.70	34.56	-0.14	[34
Hexogen (RDX)	$C_3H_6N_6O_6$	70.31	1.806	1.60	8130	7995	-135	26.90	26.61	-0.29	[34
Hexogen (RDX)	$C_3H_6N_6O_6$	70.31	1.806	1.40	7425	7387	-38	20.10	20.85	0.75	[34
Hexogen (RDX)	$C_3H_6N_6O_6$	70.31	1.806	1.20	6541	6716	175	14.50	14.44	-0.06	[34
Hexogen (RDX)	$C_3H_6N_6O_6$	70.31	1.806	1.00	5952	5949	-3	10.00	9.47	-0.53	[34
Hexogen (RDX)	$C_3H_6N_6O_6$	70.31	1.806	0.70	4765	4739	-26	4.80	4.53	-0.27	[34
Hexogen (RDX)	$C_3H_6N_6O_6$	70.31	1.806	0.56	4165	4200	35	3.30	3.03	-0.27	[34
Pentrit (PETN)	$C_5H_8N_4O_{12}$	-533.65	1.78	1.763	8270	8394	124	31.00	30.43	-0.57	[34
Pentrit (PETN)	$C_5H_8N_4O_{12}$	-533.65	1.78	1.45	7180	7220	40	20.80	19.39	-1.41	[34
Pentrit (PETN)	$C_5H_8N_4O_{12}$	-533.65	1.78	1.23	6342	6365	23	14.50	12.89	-1.61	[34
Pentrit (PETN)	$C_5H_8N_4O_{12}$	-533.65	1.78	0.99	5475	5397	-78	8.60	7.69	-0.91	[34
Pentrit (PETN)	$C_5H_8N_4O_{12}$	-533.65	1.78	0.88	5077	4965	-112.	6.90	5.96	-0.94	[34
Pentrit (PETN)	$C_5H_8N_4O_{12}$	-533.65	1.78	0.48	3631	3551	-80	2.30	1.99	-0.31	[34
Pentrit (PETN)	$C_5H_8N_4O_{12}$	-533.65	1.78	0.30	2980	3016	36.	1.10	1.00	-0.10	[34
Pentrit (PETN)	$C_5H_8N_4O_{12}$	-533.65	1.78	0.25	2830	2879	49	0.80	0.79	-0.01	[34
Trinitrotoluene (TNT)	$C_7H_5N_3O_6$	-59.35	1.654	1.64	6942	6793	-149	18.90	18.56	-0.34	[34
Trinitrotoluene (TNT)	$C_7H_5N_3O_6$	-59.35	1.654	1.45	6494	6387	-107	14.60	14.55	-0.05	[34
Trinitrotoluene (TNT)	$C_7H_5N_3O_6$	-59.35	1.654	1.36	6207	6095	-112	12.50	12.78	0.28	[34
Trinitrotoluene (TNT)	$C_7H_5N_3O_6$	-59.35	1.654	1.00	5060	5079	19	6.80	6.93	0.13	[34
Trinitrotoluene (TNT)	$C_7H_5N_3O_6$	-59.35	1.654	0.80	4423	4493	70	4.60	4.43	-0.17	[34
Tetryl (CE)	$C_7H_5N_5O_8$	33.68	1.73	1.68	7500	7507	7	23.90	23.05	-0.85	[34]
Tetryl (CE)%	$C_7H_5N_5O_8$	33.68	1.73	1.614	7479	7281	-198	22.60	21.33	-1.27	[34
Nitroglycerine (NG)	$C_3H_5N_3O_9$	-370.79	1.60	1.60	7750	7665	-85	22.00	22.22	0.22	[40]
Nitromethane (NM)	CH_3NO_2	-113.09	1.16	1.13	6350	6331	-19.	12.00	12.68	0.68	[34]
Nitric oxide (NO)	NO	79.51	1.30	1.30	5620	5499	-121	10.00	9.47	-0.53	[41]
Tetranitromethane (TNM)	CN_4O_8	37.24	1.65	1.64	6360	6361	1	15.90	14.62	-1.28	[34]
Hexanitro-ethane (HNE)	$C_2N_6O_{12}$	85.00	1.86	1.86	7580	7471	-109	-	23.27	-	[41]
Hexanitro-benzene (HNB)	$C_6N_6O_{12}$	188.00	2.02	1.973	9384	9323	-61	39.00	39.32	0.32	[41]
Benzotris-furoxane (BTF)	$C_6N_6O_6$	602.50	1.90	1.86	8490	8554	64	35.10	31.35	**-3.75**	[34
Benzotris-furoxane (BTF)	$C_6N_6O_6$	602.50	1.90	1.76	8260	8184	-76	-	28.37	-	[34
Hexanitro-azobenzene (HNAB)	$C_{12}H_4N_8O_{12}$	284.00	1.80	1.60	7310	7254	-56	20.50	22.56	2.06	[34
Diamino-dinitro ethylene (FOX-7)	$C_2H_4N_4O_4$	-134.10	1.885	1.78	8325	8527	202	28.40	30.75	2.35	[34
Diamino-trinitro benzene (DATB)	$C_6H_5N_5O_6$	-117.81	1.84	1.78	7600	7651	51	25.10	22.81	-2.29	[34
Triamino-trinitro benzene (TATB)	$C_6H_6N_6O_6$	-154.00	1.94	1.85	7660	8123	**463**	25.90	26.04	0.14	[34
Triamino-trinitro benzene (TATB)	$C_6H_6N_6O_6$	-154.00	1.94	1.50	6760	6614	-146	17.50	17.21	-0.29	[34
Nitroguanidine (NQ)/ /Estane (95%/5%)	$C_{1.246}H_{4.29}N_{3.9}O_{2.039}$	-113.88	1.727	1.704	8280	8596	**316**	26.80	26.04	-0.76	[34
Nitroguanidine (NQ)	$CH_4N_4O_2$	-95.34	1.77	1.72	8346	8799	**453**	-	27.94	-	[34
Nitroguanidine (NQ)	$CH_4N_4O_2$	-95.34	1.77	1.55	7650	7806	156	-	20.78	-	[34
Ammonium nitrate/ Fuel oil (94/6)	$C_{0.361}H_{4.442}N_{1.928}O_{2.882}$	-351.08	1.624	0.84	4740	4670	-70	6.14	4.74	-1.40	[39]
RX-23-AA (79%HyN/21%Hy)	$H_{4.551}N_{2.551}O_{1.652}$	-115.30	1.424	1.424	8580	8547	-33	20.90	22.97	2.07	[40]
RX-23-AB (69%HyN/5%Hy/26%H_2O)	$H_{3.074}N_{1.074}O_{1.557}$	-247.98	1.384	1.384	7480	7506	26	18.60	16.51	-2.09	[40]
RX-23-AC (32%HyN/68%Hy)	$H_{4.139}N_{2.139}O_{0.418}$	9.90	1.136	1.136	7870	7679	-191	16.90	15.00	-1.90	[40]
						MAE	99.5 m/s		MAE	0.89 GPa	
						MAPE	1.46 %		MAPE	6.29 %	
						RMSE	139.1 m/s		RMSE	1.21 GPa	
							1.92 %			8.07 %	

Legend: ρ_{TMD}– theoretical maximum, $D_{expt.}$ and $D_{calc.}$- experimental and calculated detonation velocities, $p_{CJ\_expt.}$ and $p_{CJ\_calc.}$- experimental and calculated detonation velocities Dif. - the difference between experimental and calculated value, MAE – mean absolute error, MAPE – mean absolute percentage error, RMSE – root mean square error

Based on the analysis of the results given in Table 4 and Fig.1, it can be concluded that there is a good agreement between the calculated and experimental values of detonation velocities (R^2=0.9996 σ=139.3 m/s, and MAPE=1.46 %). The same is evident from Fig. 2, which shows the distribution of errors. For 40 explosives out of 48 studied (83.34 %), the difference between the calculated and experimental values is below 150 m/s, which is within the measurement error. For 45 explosives (93.76%) the error is below 250 m/s (which is a bit above maximum measurement error).

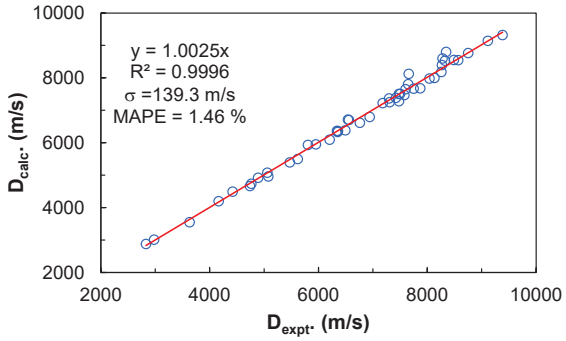

Fig. 1. Experimental *vs.* calculated detonation velocities for tested explosives

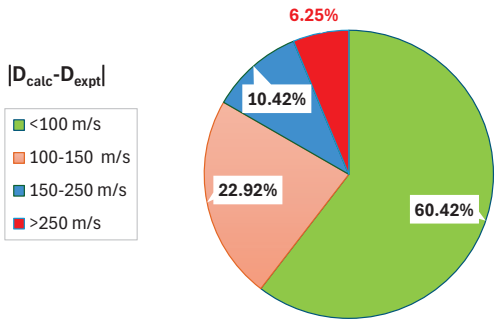

Fig. 2. Pie chart showing distribution of detonation velocity prediction errors

The difference between the measured and experimental values of detonation velocity is greater than 300 m/s (i.e. 5%) only for three explosives: TATB (+463 m/s), NQ (+453 m/s), and NQ/Estan (+316 m/s). All three explosives behave non-ideally [38], which means their detonation properties strongly depend on charge size [13]. The experimental data for NQ and TATB used in this study refer to infinite (i.e., ideal) detonation velocities, which means the value of D is obtained by extrapolating experimental D-1/d (where d is the charge diameter) dependence, obtained at smaller charge diameters, to an infinite diameter ($d \rightarrow \infty$). Extrapolating from smaller diameters to an infinite diameter may introduce an additional error, which may be the reason for the larger deviation between the calculated and experimental detonation velocities for the mentioned explosives. The following data also support the assumption that the experimental detonation velocities at infinite diameters for NQ and TATB are probably insufficiently accurate. Hobbs et al. [10] calculated detonation velocities of NQ and TATB using three different EOS and obtained significantly higher values of detonation velocities compared to the experimental (260 to 392 m/s for NQ and 469 to476 m/s for TATB) – which closely agrees with the results of this study. In addition, the calculated detonation velocity for highly non-ideal ANFO differs from the experimental infinite detonation velocity by only 70 m/s. This is most likely because the detonation velocity is measured using a huge explosive charge – about 109 tons [39], so that the diameter of the charge was close to infinity.

A comparison between the experimental and calculated values of detonation pressures is given in Figs. 3 and 4. Fig.3 shows that the calculated values are consistently a bit lower than the experimental (the slope of the line is 0.9807). For 38 explosives out of 44 tested (86.0%), the difference between the experimental and calculated pressures is less than 2 GPa, which is within the measurement error. However, MAPE is quite high (6.29%) because the error expressed in percentages is higher at lower pressures. For example, an error of 1 GPa at a pressure of 10 GPa gives a percentage error of 10%, while at a pressure of 35 GPa it gives a percentage error of 2.9%).

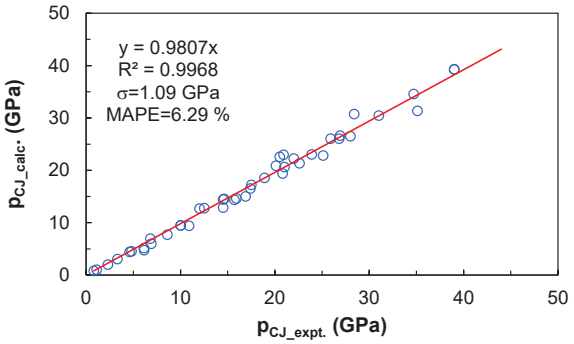

Fig. 3. Experimental *vs.* calculated detonation pressures for tested explosives

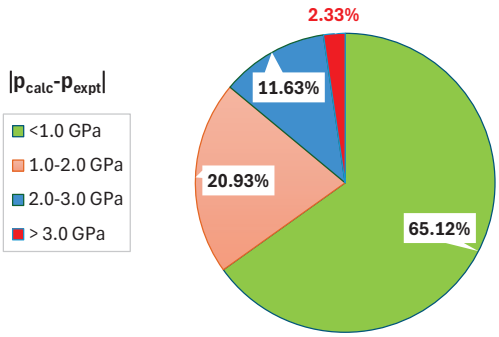

Fig. 4. Pie chart showing distribution of detonation pressure prediction errors

The difference between the measured and calculated detonation pressures is greater than 3 GPa only in the case of BTF (difference equals -3.75 GPa). Interestingly, BTF, whose detonation temperature is above 4200 K and pressure above 30 GPa, is the only one of the tested explosives to produce a diamond-like liquid carbon (other explosives produce either graphite or diamond). Thus, the larger error

in the case of BTF may be attributed to the deficiencies in the liquid carbon EOS.

Although there is not enough data for a reliable statistical analysis of the prediction errors of dCJ and pCJ for the different classes of explosives analyzed (only 6 data for non-ideal explosives and 3 data for the HNO mixture-type explosives), the analysis given in Table 5 shows that the prediction accuracy is higher for standard and well-characterized explosives than for other tested classes of explosives.

Table 5. Prediction accuracy for different classes of explosives

Explosive class	Data points*	Detonation velocity		Detonation pressure	
		MAE (m/s)	MAPE (%)	MAE (GPa)	MAPE (%)
All explosives	48/44	99.5	1.46	0.87	6.29
Standard	39/37	75.2	1.18	0.83	5.85
Non-ideal	6/4	267.5	3.50	0.65	6.96
Mixture-type (HNO)	3/3	79.7	1.01	2.02	10.79

Legend: * the first number refers to the number of experimental data for detonation velocity, second for detonation pressure

In the case of non-ideal explosives predicted detonation velocity is significantly overestimated (due to the reasons discussed previously), while in the case of HNO mixture-type explosives detonation pressure is largely overestimated. Given that HNO explosives produce a large amount of polar products, H_2O and NH_3, the reason for the discrepancy could be in an insufficiently accurate equation of state for NH_3 and H_2O (Eq. 6), especially at lower detonation temperatures.

Impact of input data on accuracy of prediction of detonation velocity and pressure

The accuracy of thermochemical calculation is influenced by the accuracy of input data on explosives (ρ_0, ΔH_f^0), the accuracy of EOS of the detonation products, and the accuracy of thermodynamic functions of the state of the detonation products. The thermodynamic state functions (*H, E, c_v, S, G*, μ, etc.) of the main detonation products, in the range 298–6000 K, are taken from the JANAF tables [33] and they are considered to be very accurate. As far as EOS gaseous detonation products are concerned, so far several authors have shown that EXP-6 EOS gives the most accurate results in a broad range of temperatures and densities [10, 11, 12, 23], provided that the interaction potential parameters (r_m, ε, α) are accurately calibrated. In this study, the values of interaction parameters are taken from several sources (Table 1). The interaction parameters for the main detonation products are calibrated based on experimental shock Hugoniots, which is considered the most accurate way to determine interaction parameters [24]. Considering the above, the impact of the accuracy of thermodynamic functions of state and EOS on the accuracy of prediction of detonation parameters are not analyzed in this paper.

Since the detonation parameters were calculated for the experimental densities (ρ_0) at which detonation velocities and pressures are measured, variations in density (i.e., measurement error) could have affected the experimental values of detonation velocities and pressures. On the other hand, inaccuracy in the enthalpy of formation values affects the calculation result. According to Rose [42] the enthalpies of formation can be determined experimentally with the measurement error of up to 20 kJ/mol. Rice et al. [43] found that the maximum difference between the enthalpies of formations derived by quantum mechanical calculations and those determined experimentally goes up to 148 kJ/mol, with RMS=37.7 kJ/mol. Given such a significant deviation, the question arises as to what is the influence of the variation of the enthalpy of formation on the calculated detonation parameters and what accuracy is required for reliable prediction of the detonation parameters. This is analysed below using RDX and PETN as examples. The detonation parameters are calculated for (ΔH_f^{298}+error), where ΔH_f^{298} are the enthalpies of formation of RDX and PETN given in Table 4 and the error varied from 20 to 100 kJ/mol). It should be noted that the influence of the enthalpy of formation on the calculated detonation parameters will be somewhat different for each explosive, depending on its composition and density. For both RDX and PETN an almost linear dependence of calculated D and p_{CJ} on ΔH_f^{298} is obtained (Fig. 5)

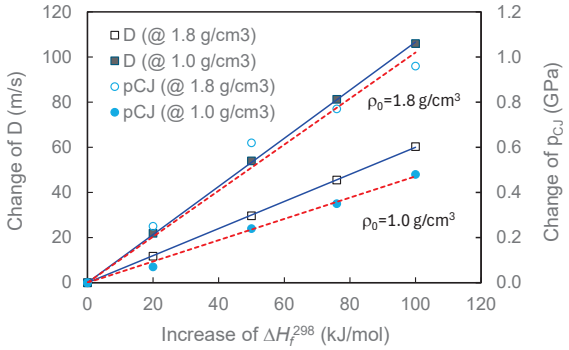

Fig. 5. Change of D and p_{CJ} at two different densities with variation of ΔH_f^{298} (note: dashed red line –p_{CJ}, solid line – D)

As follows from Fig.5, when ΔH_f^{298} increases by 100 kJ/mol, then at the density of 1.8 g/cm^3, D increases by 60 m/s (0.7%) and p_{CJ} increases by 0.96 GPa (2.8%). At the density of 1.0 g/cm^3, D increases by 106 m/s (1.8%) and p_{CJ} increases by 0.48 GPa 5.1%). In both cases, the variation of D and p_{CJ} is within measurement error (±200 m/s and ±5 GPa). Such results suggest the conclusion that ΔH_f^{298} variation has little effect on calculated D, while the effect on p_{CJ} is somewhat more significant. However, varying ΔH_f^{298} has the greatest effect on the heat of detonation (Q_d) and detonation temperature (T_d). For example, in the case of RDX, Q_d increases by about 400 kJ/kg (7%) and T_d increases by about 260 K (6.2%) when ΔH_f^{298} increases by 100 kJ/mol).

As follows from the previous discussion, different parameters affect both the experimental and calculated values of detonation velocities and pressures. When it comes to experimental results, this can result in a measurement error of several percent for detonation velocities (up to ≈200

m/s) and over 10% for pressures (up to ≈5 GPa). Such errors affect the reliability of the validation of thermochemical calculations and bring to the fore the importance of choosing accurate experimental data. Unfortunately, it is not an uncommon practice that when stating the experimental values of the detonation parameters, the authors do not provide all the necessary information (e.g., the charge size and the influence of the size on the detonation parameters, the method of initiation, measurement uncertainty, etc.).), which makes the assessment of the reliability of the results difficult. This is especially true when dealing with non-ideal explosives where the detonation parameters strongly depend on the charge size.

The results of thermochemical calculations are also affected by numerous factors, from the equation of the state of the detonation products to the charge density and enthalpy of formation. For accurate prediction of detonation parameters, it is crucial to choose an accurate equation of state, accurate enthalpies of formation of explosives, and accurate values of thermodynamic functions of the state of detonation products.

4. Conclusions

The accuracy of prediction of key detonation parameters using an analytic equation of state for EXP-6 potential fluid, incorporated in thermochemical code EXPLO5, is studied in the paper. The accuracy of prediction of detonation velocities and pressures is estimated by comparing experimental and calculated values for 48 different explosives having CHNO, CNO, HNO, and NO composition and densities in the range of 0.25-1.97 g/cm^3.

It is shown that detonation velocities for ideal explosives can be predicted with an error below 200 m/s (below 3%). The error is slightly larger in the case of NQ and TATB (which exhibit non-ideal behaviour) -predicted detonation velocities are higher by 316-463 m/s (3.9-6.0%). Statistical parameters of the correlation analysis for all 48 data points are: MAE=95.5 m/s, MAPE=1.46 %, RMSE=139.1 m/s.

The predicted detonation pressures are systematically a bit underestimated compared to the experimental (the slope of $p_{CJ\ expt.}$-$p_{CJ\ calc.}$ line equals 0.9807). Despite this, the detonation pressure can be predicted with an error of less than 2 GPa for 86% of the studied explosives, for 11.36% of the explosions the error is 2-2.5 GPa, and for only one explosive (BTF) the error is 3.75 GPa. Statistical parameters of the correlation analysis for 44 data points: MAE=0.89 GPa, MAPE= 6.29 %, RMSE=1.21 GPa.

The fact that the detonation velocity and pressure can be predicted with an error that is in most cases within the measurement error (≈200 m/s for D and ≈5 GPa for p_{CJ}), makes EXP-6 EOS suitable for application in thermochemical codes intended for detonation parameter prediction.

5. References

[1] Muravyev N. V., Wozniak D. R., Piercey D. G. Progress and performance of energetic materials: open dataset, tool, and implications for synthesis, J. Mater. Chem. A 10 (2022) 11054–11073.

[2] Wahler S., Klapötke T. M. Research output software for energetic materials based on observational modelling 2.1 (RoseBoom2. 1©), Materials Advances 3 (21) (2022) 7976-7986.

[3] Rice, B. Predicting heats of formation of energetic materials using quantum mechanical calculations. Combustion and Flame 118(3) (1999) 445–458.

[4] Chan B. High-Level Quantum Chemistry Reference Heats of Formation for a Large Set of C, H, N, and O Species in the NIST Chemistry Webbookand the Identification and Validation of Reliable Protocols for TheirRapid Computation, J. Phys. Chem. A 126 (2022) 4981-4990.

[5] Qiu L., Xiao H., Gong X., Ju X., Zhu W. Crystal density predictions for nitramines based on quantum chemistry, J. Hazard. Mater. 141 (2007) 280–288.

[6] ANSYS Autodyn Users Manual, ANSYS Inc., Release 2010;13.0.

[7] LS-DYNA Theory Manual, ANSYS Inc., 2002.

[8] Fried, L. E., Howard W. M., Souers P. C. Cheetah 2.0 user's manual. (UCRL-MA -117541). Energetic Materials Center, Lawrence Livermore National Laboratory, Livermore, 1998.

[9] Suceska M. EXPLO5-Users's guide, OZM Research, Hrochuv Tynec, Czech Republic, 2018.

[10] Hobbs, M. L., Brundage A. L., Yarrington C. D. JCZS2i: An Improved JCZ Database for EOS Calculations at High Temperature and Pressure, 15th Symposium (International) on Detonation (Office of Naval Research, San Francisco, CA, 2014, 804-8012.

[11] Victorov S. B. and Gubin S. A. A new accurate equation of state for fluid detonation products based on an improved version of the KLRR perturbation theory, 13th International Detonation Symposium, Ed. S. M. Peiris, Norfolk, Virginia, USA, 2006, 1118-1127.

[12] Dubois V., Desbiens N., Auroux E. New developments of the CARTE code: Calculation of detonation properties of high explosives, Chem. Phys. Lett. 494 (2010) 306-311.

[13] Mader C.L. Numerical modeling of explosives and propellants, CRC Press, Boca Raton, 2008.

[14] Fickett W., Davis W. C. Detonation: Theory and Experiment, Dover Publication, Mineola, N.Y., 1979.

[15] Wood W.W., Kirkwood J. Diameter effect in condensed explosives: the relationship between velocity and radius of curvature of the detonation wave, J. Chem. Phys. 22(11) (1954) 1920-1924.

[16] Kamlet M. J., Jacobs S. J. Chemistry of Detonations. I. A., Simple Method for Calculating Detonation Properties of C–H–N–O Explosives, J. Chem. Phys. 48 (1968) 23–35.

[17] Keshavarz M. H., Zamani A. A Simple and Reliable Method for Predicting the Detonation Velocity of CHNOFCl and Aluminized Explosives, Central European Journal of Energetic Materials 12(1) (2015) 13-33.

[18] Bastante F. G., Araujo, M. Giraldez G. Predictive model of explosive detonation parameters from an equation of state based on detonation velocity, Phys. Chem. Chem. Phys. 24 (2022) 8189-8195.

[19] Liu W-H., Liu Q-J., Liu F-S., Liu Z.-T. Machine learning approaches for predicting impact sensitivity and detonation performances of energetic materials, J. Energy Chem. 102 (2025) 161-171.

[20] Davis J. V., Marrs F. W., Cawkwell M. J., Manner V. W. Machine Learning Models for High Explosive Crystal Density and Performance, Chem. Mater. 36(22) (2024) 11109-11118.

[21] Rossi, C.C.R.S., Lorenzo-Filho L., Guirardello R. Gibbs free energy minimization for the calculation of chemical phase equilibrium using linear programming, Fluid Phase Equilibria 278 (2009) 117-128.

[22] White, W.B., Johnson, S.M., Dantzig, G.B., Chemical equilibrium in complex mixtures, J. Chem. Phys. 28(5) (1958) 751-755.

[23] Fried L. E., Howard W. M., Souers P.C. EXP6: A new equation of state library for high-pressure thermochemistry, 12th International Detonation Symposium, Ed. J. Short. Arlington, VA, San Diego, California, USA, August 11–16, 2002, 564-575.

[24] Suceska M., Braithwaite M., Klapotke T., Stimac B. Equation of State of Detonation Products Based on Exponential-6 Potential Model and Analytical Representation of the Excess Helmholtz Free Energy, Propellants Explos. Pyrotech. 44(5) (2019) 1–9.

[25] Byers Brown V. Analytical representation of the excess thermodynamic equation of state for classical fluid mixtures of molecules interacting with α-exponential-six pair potentials up to high densities, J. Chem. Phys. 87 (1987) 566-577.

[26] Ree F.H. J. A statistical mechanical theory of chemically reacting multiphase mixtures: Application to the detonation of PETN, Chem. Phys. 81(3) (1984) 1251-1263.

[27] Charlet F., Turkel M.L., Danel J.F., Kazandjian L.J. Evaluation of various theoretical equations of state used in calculation of detonation properties, J. Appl. Phys. 84(8) (1998) 4227-4238.

[28] McGee B. C., Hobbs M.L., Baer M. R., Exponential 6 Parameterization for the JCZ3-EOS, Report SAND98-1191, Sandia National Laboratory, USA, 1998.

[29] Victorov S. B., El-Rabii H., Gubin S. A., Maklashova I. V., Bogdanova Y. A. An accurate equation of state model for thermodynamic calculations of chemically reactive carbon-containing systems, J. Energ. Mater. 28 (2010) 35–49.

[30] Braithwaite M., Allan N. L. Thermodynamic representations for solid products in ideal detonation predictions, 12th International Detonation Symposium, Wyndham San Diego at Emerald Plaza, California 92101, August 11 - 16th, 2002, 601-607.

[31] Fried L. E., Howard W. M. Explicit Gibbs free energy equation of state applied to the carbon phase diagram, Physical Review B 61 (13) (2000 8734-8743.

[32] Victorov S. B., Gubin S. A., Maklashova I. V., Pepekin V. I. Predicting the detonation characteristics of hydrogen-free explosives. Khimicheskaya Fizika 24 (2005) 22–45.

[33] Chase M. W., Davies C. A., Downey J. R., Frurip D. J., McDonald R. A., Syverud A. N. JANAF Thermochemical Tables, Third Edition, J. Phys. Chem. Ref. Data, Vol. 14, Suppl. 1,1985.

[34] Hobbs M. L., Baer M. Calibrating the BKW–EOS with a Large Product Species Data Base and Measured C–J Properties, Tenth Symposium (International) on Detonation, Boston, Massachusetts, July 12 - 16, 1993, 409-418.

[35] Chirat R., Pittion-Rossillon G. Detonation properties of condensed explosives calculated with an equation of state based in intermolecular potential, Seventh Symposium (International) on Detonation, Annapolis, Maryland, June 16-19, 1981, 703-715.

[36] Suceska M. Test methods for explosives, Springer-Verlag, New York, 1995.

[37] Kamlet M. J., Dickinson C. Chemistry of Detonations. III. Evaluation of the Simplified Calculational Method for Chapman–Jouguet Detonation Pressures on the Basis of Available Experimental Information, J. Chem. Phys. 48 (1968) 43–50.

[38] Fried L.E., Clark Souers P. BKWC: An Empirical BKW Parametrization Based on Cylinder Test Data Propellants, Explos., Pyrotech. 21 (1996) 215-223.

[39] Helm F, Finger M, Heyes B, Lee E, Chueng H, Walton J. High explosive characterization for the dice throw event. Lawrence Livermore National Laboratory; 1976. Report UCRL-52042.

[40] Kerley G. I., Christian-Frear T. L. Prediction of explosive cylinder test using the equation of state from the PANDA code, Report SAND-93-2131, Sandia National Laboratory, New Mexico, USA 1993.

[41] Victorov S. El-Rabii B., Gubin H., S. A., Maklashova I. V., Bogdanova Y. A. An accurate equation of state model for thermodynamic calculations of chemically reactive carbon-containing systems, J. Energ. Mater. 28 (2010) 35–49.

[42] Rouse P. E. Enthalpies of Formation and Calculated Detonation Properties of Some Thermally Stable Explosives, Journal of Chemical and Engineering Data 21(1) (1976) 16-20.

[43] Rice B. M., Pai S. V., Hare J. Predicting Heats of Formation of Energetic Materials Using Quantum Mechanical Calculations, Combustion And Flame 118 (1999) 445–458.

Thomas M. Klapötke [1]

New Secondary Explosives and Oxidizers: TKX-50 and TNEF

[1] Ludwig-Maximilian University of Munich (LMU), 81377 Munich, Germany

Abstract

The energetic materials research group at LMU has been interested in the synthesis and energetic properties of new explosives and rocket propellant ingredients for many years. Out of the many interesting compounds which we have prepared over the years, the most promising candidate compound for use in real-life applications is the secondary explosive TKX-50. An overview of the synthesis and properties of TKX-50 will be given, as well as recent aspects we have investigated. The progress and development of new CHNO-based oxidizers will also be discussed, focusing predominantly on 2,2,2-trinitroethyl formate (tris(2,2,2-trinitroethyl)orthoformate, TNEF).

Keywords: *Secondary explosives, oxidizers, TKX-50, BTNEO, TNEF*

1. Introduction

Within the area of secondary explosives, the major topics and challenges of today are to find compounds which can be prepared on an industrial scale for use as secondary explosives which have – in addition to the standard properties every secondary explosive must possess – (i) higher performance than current state-of-the-art secondary explosives, (ii) higher insensitivity (i.e. lower sensitivity) to external stimuli such as impact, friction or electrostatics and (iii) lower toxicity and higher environmental compatibility.

If these goals are considered in more detail, it is clear that a higher performance is always advantageous. Higher performance means that the secondary explosive shows higher values for detonation velocity, detonation pressure and heat of detonation. In particular, for new secondary explosives, it is important to increase performance specifically in the areas of blast effect (for destructive effect), metal acceleration, and with respect to shaped charges. In the field of secondary explosives, performance is closely associated with the following parameters, all of which can be predicted using the EXPLO5 [https://www.ozm.cz/explosives-performance-tests/thermochemical-computer-code-explo5/] thermochemical computer code [1], or measured experimentally: (i) detonation velocity ("velocity of detonation," VoD in ms^{-1}), (ii) detonation pressure ("Chapman-Jouguet pressure," p_{C-J} in GPa) and (iii) detonation heat (Qex in $kJkg^{-1}$) ([2], [3], [4], [5], [6], [7], [8], [9], [10], [11], [12], [13], [14], [15]). The large samples required and difficulties in measuring parameters such as VoD and p_{C-J} experimentally mean that the energetic performance parameters of new secondary explosives are always calculated in the first instance, and only the most promising candidate compounds are prepared on a larger scale for testing.

Reduced sensitivity is an aspect which is particularly important in the areas of mechanical sensitivity (bullet impact), greater thermal stability (fuel fires), and tandem-shaped charges (two shaped charges placed in sequence). In each of these areas, the aim is to prevent unintended and unwanted detonation of a secondary explosive due to initiation caused by sensitivity of the secondary explosive to an external stimulus such as impact or heat. This is vital in improving safety, and also in widening the work-range a secondary explosive can be used in. Reduced toxicity and lower environmental impact refer not only to the explosive itself, but also to its detonation products, as well as its degradation products in the environment. In addition, reduced toxicity can also be applied to the production of the explosive which should not involve any toxic chemicals or produce any toxic by-products in the process. Ideally, the improved secondary explosive should be able to be produced in a procedure which is resource economical and doesn't "waste" chemicals. RDX (Hexogen) is one of the most commonly used military explosives, and has been used for decades for military applications. RDX is cheap to synthesize and shows very good energetic performance (pure RDX: VoD = 8833 ms^{-1}, p_{C-J} = 33.6 GPa, Q_{ex} = –5740 $kJ\ kg^{-1}$). However, RDX is relatively impact sensitive (7.5 J) and friction sensitive (120 N), which means that it doesn't show ideal values for safe handling. A further long-term issue with RDX is that it is toxic to both humans and the environment (the recommended limit in groundwater is a maximum of 2 $\mu g\ L^{-1}$) [11], which is a significant problem especially when considering the large scale on which it is produced. There are in addition, many more complex issues with current secondary explosives with respect to their application in specific situations. The problems outlined above for secondary explosives have acted as the motivation for the energetic materials research group at LMU Munich to strive towards the goal of developing new, even more powerful, less sensitive, and more ecologically and toxicologically compatible secondary explosives.

2. Design of new explosives

An ideal explosive must be designed in which many factors have been incorporated into the molecule. One of the most important of these is that the oxidizer (e.g. nitro groups, $-NO_2$ present) and the fuel (e.g. the carbon framework) are combined within the same molecule. This is the case, for example, in TNT, where the three nitro groups act as the oxidizer and the carbon-hydrogen framework provides the oxidizable component, i.e. the fuel. It is important for such molecules to be as endothermic as possible, since more

energy will then be released on detonation. Molecules such as TNT in which nitro groups are attached to a carbon framework can be made even more endothermic by altering the valence angles of the carbon atoms. Usually, tetrahedral carbon atoms have angles of ca. 109.5°. However, by forming rings or cages, the arrangement of atoms/groups around carbon atoms can be engineered to deviate significantly from this value, resulting in strain which contributes to increasing the endothermicity of the molecule. This is the case for two prominent secondary explosives. For example, octanitrocubane is a compound in which eight nitro groups are attached in total to the corners of cubane, meaning that each carbon atom in ONC has three 90° bond angles and is attached to three C atoms and one -NO_2 group. A consequence of the difficult synthesis of ONC - which has only produced ONC in very small quantities so far - is that it has not been investigated for use and remains currently of academic interest. Perhaps the best-known example of a secondary explosive which has a cage structure is CL-20 (Figure 1). Despite being one of the best-known non-nuclear explosives and having been developed around 30 years ago at the Naval Air Warfare Center China Lake, CL-20 has not yet found widespread use. This is due to both the high cost of the compound and its relatively high sensitivity towards external stimuli. A further issue that plagues CL-20 is polymorphism – unfortunately CL-20 exists in different polymorphs in temperature regions relevant to its use in the field. Phase changes are undesirable, since different phases can show different densities and specific volumes [11].

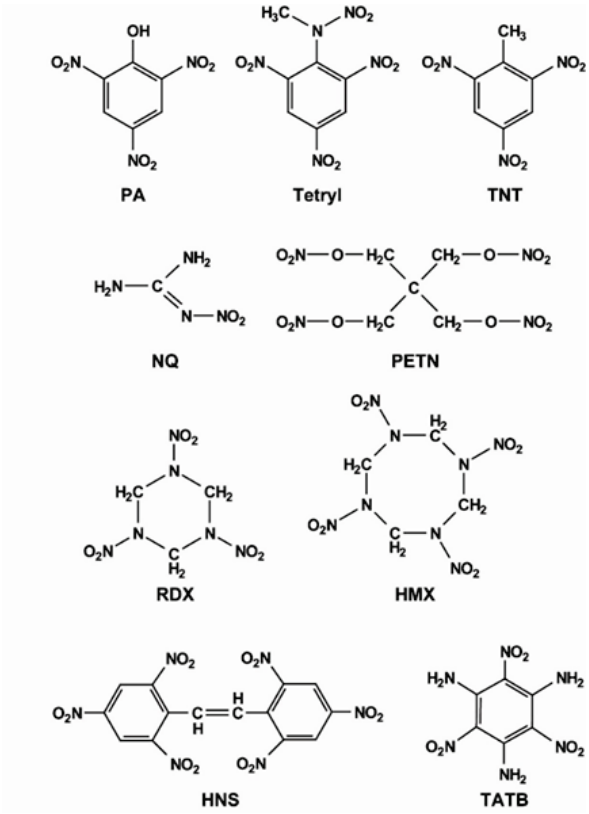

Fig. 1. Molecular structures of some secondary explosives

The synthesis of nitrogen-rich molecules follows a completely different concept ([16], [17], [17], [18], [19], [20], [21]). Nitrogen is unique in the periodic table in that the average bond energy per 2-electron bond increases from single to double to triple bonds (Figure 2), while the opposite is true for its neighboring element, carbon. Thermodynamically, acetylene (C_2H_2) would be expected to trimerize into benzene (C_6H_6), however, N_2 (isolobal to acetylene) would never be expected to trimerize at room temperature to form hexaazabenzene (N_6) [11].

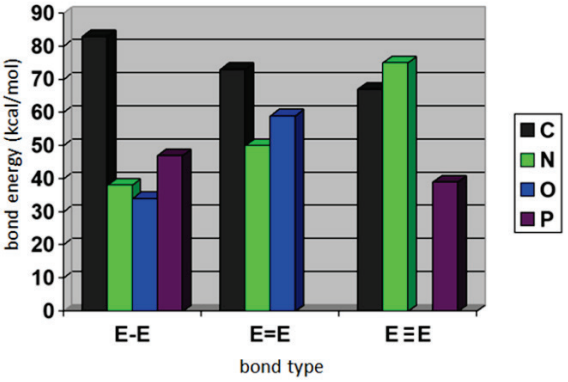

Fig. 2. Average element-element bond energies per 2-electron bond (in kcal mol-1).

Due to nitrogen showing the opposite trend in average bond energies per 2-electron bond (bond energies: C-C > C=C > C≡C but N-N < N=N < N≡N), any N-N bonds present in a molecule release a considerable amount of energy when they are converted into N≡N bonds in N_2. For this reason, nitrogen-rich molecules (N > 60%) with average N-N bond orders of < 2 are particularly of interest in the design and synthesis of new high-energy secondary explosives [11]. Even if a molecule has a high nitrogen content of 60% or 70%, and only few C-H units are present, these C-H units must be oxidized during the detonative process, and in order for this to occur, oxidizing groups, as are shown in Figure 3, must be present in the molecule. In order to oxidize one >CH_2 group, one -NO_2 group is required to convert the carbon into CO and the two hydrogen atoms into H_2O [11].

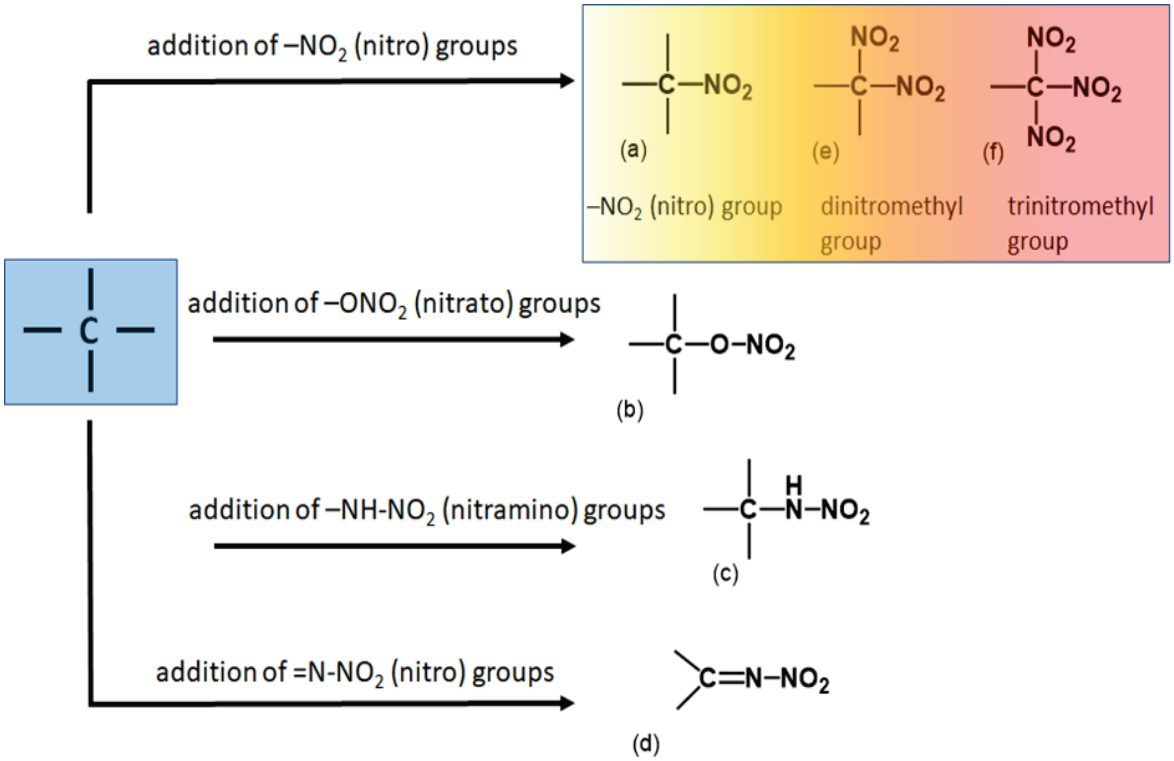

Fig.3. Possibilities for introducing oxidizing groups into an energetic material: a) nitro, b) nitrato, c) nitramino, d) nitrimino, e) dinitromethyl, f) trinitromethyl.

In addition to introducing oxidizing groups into a nitrogen-rich molecule, the oxygen balance of a molecule can be improved by incorporating the N-oxide or the N-O functionality. The oxygen balance describes the relative amount of oxygen excess or deficit (with negative sign "–"), to achieve a balanced ratio between the oxidizer and the combustible components (fuel). Therefore, the addition of oxygen to a trivalent nitrogen atom to convert it into an N-oxide functional group is an excellent possibility to increase the oxygen balance of the molecule, but without adding any other undesirable elements. Improving the oxygen balance is not the only reason that N-oxides have become popular target compounds. It has been observed that N-oxides generally show higher densities than the corresponding compound without the N-O group, which has been attributed to increased polarity of the N-oxides, due to the stronger intermolecular attraction associated with the >N+-O- group (Equation 1) [11]:

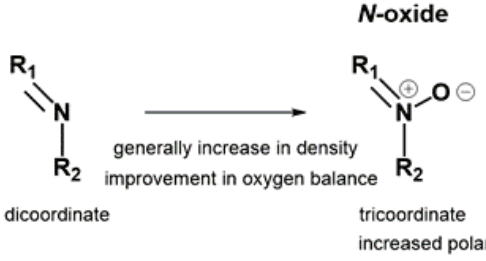

(1)

A high density is important for energetic materials, since the detonation velocity is proportional to the density, while the detonation pressure is even quadratically proportional to the density (Equations 2 and 3). This means that the incorporation of the N-oxide group which generally results in an increase in the density is also advantageous in this sense too.

$$P_{C-J} \propto \rho^2 \quad (2)$$

$$VoD \propto \rho \quad (3)$$

In terms of improving the stability of a secondary explosive, there are several approaches - and combinations thereof - which can be adopted, depending on whether the secondary explosive target compound is a neutral molecule or a salt. The three principal methods which are generally used are: (i) incorporation of a so-called push-pull mechanism, in which -NH_2 groups donate electrons into the system which are pulled by neighboring -NO_2 groups, (ii) stabilization through formation of π-delocalization or conjugation and (iii) formation of a salt instead of a neutral molecule, in order to increase stabilization due to the lattice energy. Examples of successful energetic push-pull system molecules are Fox-7 ($(H_2N)_2C{=}C(NO_2)_2$) or triaminotrinitrobenzene (TATB). A highly stable secondary explosive which is stabilized through π-delocalization is hexanitrostilbene (HNS). Fox-7, TATB and HNS are all used in military applications. One of the most exciting new secondary explosives to appear on the scene is dihydroxylammonium-5,5′-bistetrazolyl-1,1′-diolate (TKX-50) which is a salt, in contrast to the neutral molecules Fox-7, TATB and HNS. TKX-50 incorporates not only the nitrogen-rich and N-oxide formation strategies mentioned above, it also benefits in terms of stability from π-delocalization within the anion, and the lattice energy involved with being a salt.

3. Secondary explosives

Since TKX-50 is clearly one of the most promising new secondary explosives to have emerged in recent years, it is worth looking at why this is so in more detail. TKX-50, (Dihydroxylammonium-5,5′-bistetrazolyl-1,1′-diolate, Fig. 4, Tab. 1) was first synthesized in the energetic materials group at LMU Munich and published in 2012 ([22], [23], [24]). The potential of TKX-50 was immediately indicated by the energetic performance parameters which were predicted using the thermochemical computer code EXPLO5 [1], in combination with its sensitivity to external stimuli which were determined experimentally. Based on this initial selection criteria, TKX-50 immediately became of considerable interest for further examination and testing.

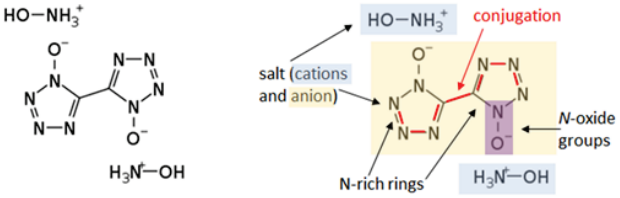

Fig. 4. Structure of dihydroxylammonium-5,5′-bistetrazolyl-1,1′-diolate, TKX-50

Table 1 shows that the density of TKX-50 at room temperature is high (1.877 gcm^{-3}) and the compound is endothermic with an enthalpy of formation of 197.4 kJ mol^{-1} [26]. The decomposition temperature is above 200°C which is good, and the sensitivity of TKX-50 to impact, friction and electrostatic stimuli all lie within accepted ranges for secondary explosives. The oxygen balance with respect to CO_2 (ΩCO_2) is only -27.1 % which is quite low, and is a consequence of the presence of two carbon atoms and 8 hydrogen atoms per salt equivalent and the absence of any oxidizing groups such as -NO_2, with only two N-oxide functional groups being present instead. Despite this, the energetic performance parameters of TKX-50 (VoD = 9649 ms^{-1}, p_{C-J} = 37.1 GPa, Qex = 4791 kJmol^{-1}) are excellent being superior or comparable than those of RDX (VoD = 8877 ms^{-1}, p_{C-J} = 34.5 GPa, Q_{ex} = 5745 kJmol^{-1}) and HMX (VoD = 9192 ms^{-1}, p_{C-J} = 37.8 GPa, Q_{ex} = 5699 kJmol^{-1}) (always at TMD).

Table 1. Structure of dihydroxylammonium-5,5′-bistetrazolyl-1,1′-diolate, TKX-50

Formula	$C_2H_8N_{10}O_4$
M/gmol^{-1}	236.2
IS/J	8 – 18
FS/N	120
ESD/J	0.1
$\Omega(CO_2)$/%	-27.1
T_{dec}/°C	crude: 221 recryst. from water: 237
ρ/gcm^{-3}	1.918 @ 100 K 1.877 @ room temperature
$\Delta H°_f$/kJmol^{-1}	197.4 mol^{-1}* (Paraskos, 2016, Schaller, 2020, Silva, 2023, Sinditskii, 2015,) 213 ± 20 kJ mol^{-1}(Klapötke, 2022) 175.3 ± 1.9 kJ mol^{-1} (Silva, 2023)

The original synthesis of TKX-50 was based on the N-oxidation of a C-C-linked bistetrazole, followed by the chromatographic separation of the formed isomers (Fig. 5). The N-oxide group was introduced using the oxidizer Oxone, which is the triple salt $2KHSO_5 \bullet KHSO_4 \bullet K_2SO_4$ which contains the active oxidizer potassium peroxymonosulfate, $KHSO_5$ [11].

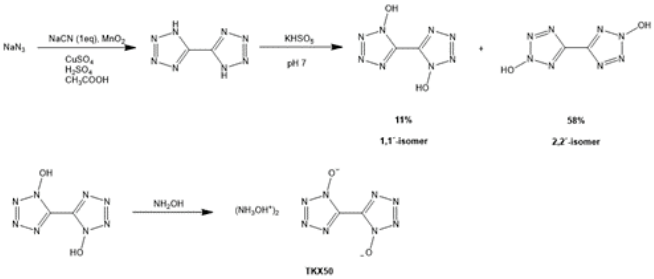

Fig. 5. Originally published synthesis of TKX-50 ([22], [25]).

Despite being a successful synthesis in the lab on very small scales, this method was not suitable for scale-up due to the separation of the isomers requiring column chromatography. Therefore, because of the promising properties that TKX-50 showed, considerable effort was invested into developing a new synthesis which was based on the chlorination and subsequent cyclization of glyoxime as shown in Fig. 6 and which would eliminate the problematic step.

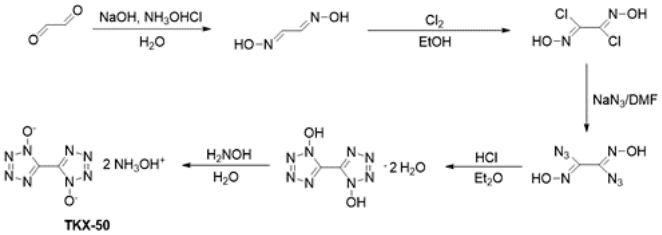

Fig. 6. Synthesis of TKX-50 starting from glyoxal ([23], [24]).

The second method shown in Fig. 6 avoids various isomers of the diole being obtained, which require separation. However, the synthesis in fig. 6 also has issues, since it requires isolation of diazidoglyoxime as an intermediate, and this compound, has the sensitivity of a primary explosive (IS = 1.5 J, FS <5 N, ESD = 76 mJ) and was therefore also not suitable for scale-up. The formation of

intermediates or by-products which have the sensitivities of primary explosives makes a synthetic method unsuitable for safety reasons, since primary explosives are much more sensitive to impact, friction and electrostatic discharge than secondary explosives are (typical values for primary explosives: IS = <4 J, FS = <10 N, ESD = 0.002 – 0.02 J). A further drawback of this synthetic route is the requirement of the gases chlorine (Cl2) and HCl which would also have been an obstacle to industrial production.However, in order to a secondary explosive to have a future for industrial production, a suitable synthetic route must be found. For TKX-50, another synthetic route was again developed by the energetic material group at LMU, which produces TKX-50 starting from commercially available glyoxime in the one-pot, 4-step reaction shown in Fig. 7 in an overal yield of approximately 85%. This synthetic route achieves the synthesis of TKX-50 from cheap, commercially available starting materials, in high yields, without requiring any explosive intermediates or separation of isomers, and also avoids the use of any gaseous reactant or toxic solvents ([27]). The ability to produce TKX-50 through such a route was a further milestone in the journey of TKX-50 from laboratory compound to possible industrial production.

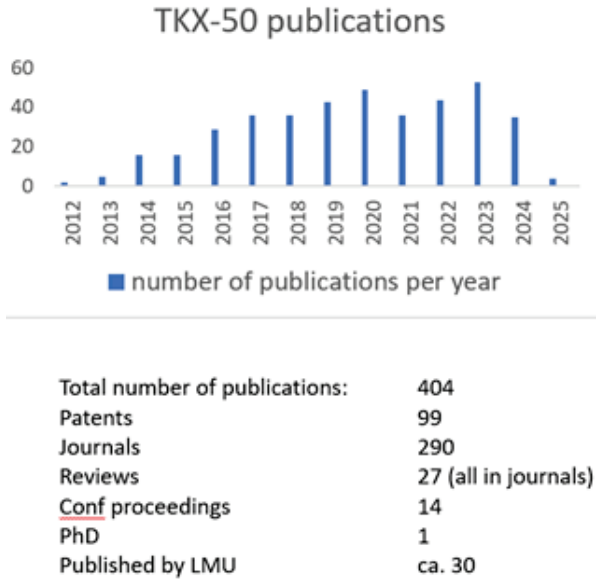

Fig. 8. Publications on TKX-50 up to January 2025.

The suitability of TKX-50 for application as a secondary explosive in warheads, shaped charges and similar applications has been a major focus of the published articles ([28], [29], [30], [31], [32], [33], [34], [35], [36], [37], [38], [39], [40]). A further aspect which has also received a lot of attention is the suitability of TKX-50 as an ingredient in solid rocket propellants has been studied extensively ([28], [41], [42], [43]). More recently, focus has been directed to the possibility of using TKX-50 in thermobaric compositions, and various theoretical and experimental investigations have been reported [44].

Recently, the behavior of TKX-50 in model thermobaric formulations was reported in which Aluminum was added to TKX-50 (Fig. 9). Experimental investigations were able to show that the addition of about 10% Al to TKX-50 resulted in a decrease in Qdet by about 90 Jg^{-1}. However, Al reacts with the detonation products of TKX-50 in an exothermic manner, and this energy contribution was calculated to be approximately 375 Jg^{-1}. A thermobaric mixture of TKX-50 charges containing 27% Al was shown to detonate, generating an overpressure in the argon-filled explosion chamber that was approximately 20% higher than that observed for only pure TKX-50 (Tab. 2). A 370 K higher maximum temperature of the TKX-50/Al explosion products in the argon-filled chamber was also observed for the thermobaric mixture than that measured after detonating only TKX-50. Aluminum oxynitride with a low nitrogen content has been found in the solid detonation products of aluminized TKX-50, but only when detonated in argon. When detonated in an air atmosphere, charges of the TKX-50/Al mixture generate significantly higher overpressure and radiant temperature values. Overall, burning aluminum in nitrogen provides little energy, and even if the concentration of nitrogen in the post-detonation products is much higher than that of oxygen, aluminum oxides are still preferentially formed (Fig. 9 and 10) [44].

Fig. 9. TKX-50 charge metallized with Al (left) and witness plate after detonation of the TKX-50/Al charge (right) (Klapötke, 2023).

The experimentally determined values for the maximum overpressure in the detonation chamber filled with air or with argon for pure TKX-50 and the thermobaric mixture of TKX-50/Al are summarized in table 2.

Table 2. Measured and calculated values for the maximum overpressure in the chamber [44].

	TKX-50		TKX-50/Al	
	Air	Ar	air	Ar
Δp_{max} [MPa]	0.63	0.48	0.81	0.58
Δp_{cal} [MPa]	0.97	0.70	1.14	0.92
$\Delta p_{max}/\Delta p_{cal}$ [%]	65	69	71	64

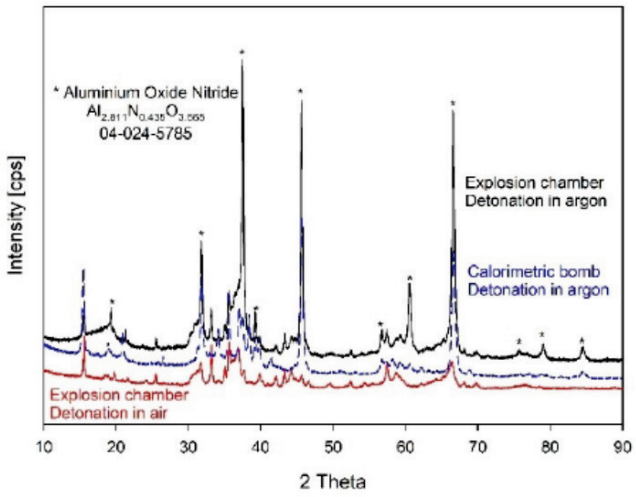

Fig. 10. XRD patterns of the solid detonation products of aluminized TKX-50 obtained in an Ar atmosphere (black and blue) and in an air atmosphere (red) [44].

Overall, it was found that a TKX-50 charge metallized with Al detonated in air shows a detonation pressure which is higher than if TKX-50 is detonated without Al. It is also the case, that a TKX-50 charge metallized with Al detonated in an argon atmosphere also shows a higher pressure than detonation of TKX-50 detonated in argon without Al [44].

Of the many challenges involved in investigating the properties of TKX-50, one challenge which posed many issues was determining the enthalpy of formation of TKX-50. The enthalpy of formation of TKX-50 was a source of debate in the literature until recently, when finally, a series of values indicated that the enthalpy of formation of TKX-50 is in the range of 175.3 kJ mol-1 (Silva, 2023) - 213 kJ mol^{-1} [45]. The average value for the enthalpy of formation of solid TKX-50 based on the combustion calorimetry measurements of several independent research groups is 197.4 kJ mol-1 ([26], [46], [47], [48]). Prior to the most recently measured enthalpy of formation value for TKX-50, the best experimentally determined value for the enthalpy of formation of solid TKX-50 using combustion calorimetry was $\Delta H°_f$(TKX-50, s) = 213 ± 20 $kJmol^{-1}$ [45] and was used for the following energetic performance data calculations. However, more recently, the value of 197.4 $kJmol^{-1}$ has been used instead and is currently the recommended value for the enthalpy of formation of solid TKX-50 [26].

As was stated previously, an accurate value for the enthalpy of formation is essential for predicting the energetic performance parameters of an energetic material. If a value for the enthalpy of formation is used which is too high, the VoD and pC-J will be predicted too high. Using the improved value for the enthalpy of formation of TKX-50 in the solid state [26] allowed the performance parameters of TKX-50 to be calculated, and be compared with the values which were recently determined experimentally. Not only is good agreement observed for the calculated and experimentally determined performance parameters, some of the values for TKX-50 exceed those of currently used secondary explosives (Tab. 3) [26]. Determination of the detonation velocity experimentally is not a trivial task, particularly for TKX-50, which has a large critical diameter. A consequence of this is that a large quantity of TKX-50 is required using a larger-scale experimental set-up [45] based on the short-circuit method (Figs. 11 and 12). The previously reported value for the detonation velocity of TKX-50 that had been determined experimentally was obtained using the LASEM method, which is a completely different approach requiring only a single crystal in contrast to the multigram quantities required for the more standard method that was more recently used ([49], [50], [51], [52], [53]).

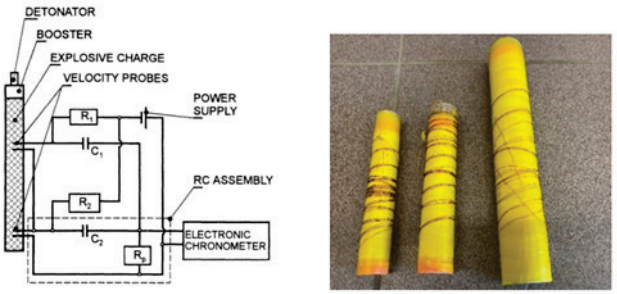

Fig. 11. A set of short-circuit items for measuring the detonation velocity of TKX-50 (left) and a schematic presentation of the short-circuit method which was used (right) [45].

Fig.12. Samples of TKX-50/Paraffin 97/3 granules before drying (left) and a set of pressed pellets of the same formulation (right) [45].

In the recent past, progress has also been made in obtaining more data regarding the sensitivity of TKX-50 to external stimuli. The most important physical data of TKX-50 are summarized in Tab. 3 for both the crude product, as well as for TKX-50 which was recrystallized from water. The basic sensitivity data which are generally presented for new secondary explosives are the impact and friction sensitivities as well as the sensitivity to electrostatic discharge. However, for compounds which show particular promise, there are many other sensitivity and stability data which must be determined, such as the long-term thermal stability, compatibility with relevant compounds and its performance in the slow cook-off as well as Koenen tests. All of these tests have been reported meanwhile for TKX-50. Furthermore, the performance of TKX-50 in model thermobaric formulations has also been very recently investigated in mixtures of TKX-50 with 10% micron-sized

aluminum powder (TKX-50/Al, 90/10) and 27% Al powder (TKX-50/paraffin/Al, 70/3/27) [44].

Table 3. Calculated performance parameters of TKX-50 compared to that of other secondary explosives ([45], [1]).

Explosive	ρ / gcm^{-3}	HE : wax	VoD / ms^{-1}	$p_{C\text{-}J}$ / GPa	Q_{det} / kJkg^{-1}
TKX-50	1.74	97 : 3	8919	30.0	4627
	1.877 (TMD)	100 : 0	9649	37.1	4791
RDX	1.74	97:3	8490	30.2	5561
	1.82 (TMD)	100	8877	34.5	5745
HMX	1.74	97:3	8472	29.9	5502
	1.905 (TMD)	100	9192	37.8	5699
CL-20	1.74	97:3	8506	31.4	5855
	2.038 (TMD)	100	9773	44.7	6231

The detonation characteristics of several explosive formulations based on TKX-50 have also been calculated, in which materials such as paraffin, HTPB, GAP, AMMO and BAMO were considered as fillers or binders ([35], [36], [37]). The influence of such fillers (with a volumetric content of up to 50%) on the detonation characteristics of the composite energetic materials was investigated (Fig. 13). In addition, the influence of porosity on the detonation characteristics of composite explosive formulations with a binder mass content of 5 and 10% has also been determined. The experimentally determined detonation velocities of three explosive formulations with inert and energetic binders showed good agreement could be observed between the calculated and experimental results for the detonation velocity (Fig. 14). A computational study of the explosion impact of charges of TKX-50 - as well as of explosive formulations based on TKX-50 containing the binders HTPB, GAP, AMMO and BAMO with 5% mass content of binder - on copper plates with a thickness of 1 mm and on layers with a thickness of 50 mm has also been reported. The charges (50 mm thick) and consisted of compact or porous materials with a porosity of 2% (Fig. 15). The EXPLO5 and Ansys Autodyn programs performed the thermochemical, thermodynamic and gas-dynamic calculations.

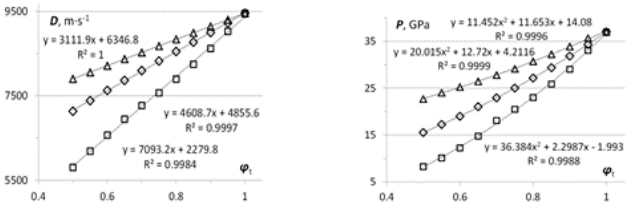

Fig. 13. Calculated values showing the influence of the volumetric content of TKX-50 on the detonation velocity (left) and detonation pressure ($p_{C\text{-}J}$) (right) of the energetic material TKX-50 (squares), as well as of the composite energetic materials with paraffin (rhombuses) and GAP (triangles) [37].

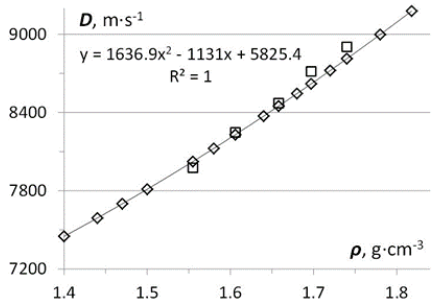

Fig. 14. Influence of the density of composition 1 (97% TKX-50 and 3% paraffin) on the detonation velocity: rhombuses - calculation, squares - experiment [37].

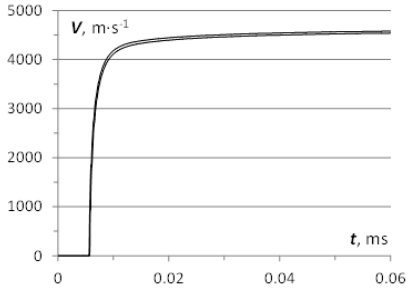

Fig. 15. Velocities of copper plates (1 mm thick) under explosive loading with charges with a paraffin binder (5%) 50 mm thick and a relative density of 100 and 98% ([18], [37]).

Moreover, a small-scale shock reactivity test (SSRT) was performed (Tab. 4), and the values of the relative dent size of TKX-50 were in good agreement with the calculated cylinder energies (Tab. 5) ([54], [55]).

The SSRT test procedure used is described in detail in the literature ([54], [55]) and is therefore only summarized here. An aluminium cylinder and steel cylinder (both 25.0 mm x 50.0 mm) are placed on top of each other (steel cylinder on top) and held together using crepe tape. The steel cylinder has a 7.5 mm hole from top to bottom in the center of the cylinder. A specific quantity of the explosive substance being tested is then filled into this hole and subsequently pressed by placing a steel pin (7.45 mm diameter) into this hole and pressing using a hydraulic press with 3 tons pressure. After repeating the pressing procedure twice, and removal of any explosive material residue in the hole after pressing and removal of the steel pin, the hole was cleaned

using a pipe-cleaner. The cylinder construction was then placed in a steel apparatus as is illustrated in reference [54], a Danadet-C2 detonator placed into the hole in the steel cylinder and initiated. The size of the dent resulting from the explosion was then measured using a profilometer. This procedure was performed twice per sample ([54], [55]).

Tab. 4. Results of a small-scale shock reactivity test (SSRT) showing the relative dent size of the tested compounds with respect to each other.

Explosive	mass [mg]	rel. dent size [volume in %]
RDX	504	69
CL-20	550	110
TKX-50	509	102

Tab. 5. Calculated cylinder energiesfor TKX-50 and RDX.

		% of standard			
compound	E_C / kJTATB cm^{-3}	PETN	HMX	Cl-20	
V/V_0					
TKX-50					
2.2	–8.16	168	128	109	90
RDX					
2.2	–6.94	143	109	93	77

Since the long-term stability is clearly an important factor when considering whether an energetic material is suitable for real-life applications, the stabilities of four commonly-known secondary explosives with real-life applications (RDX, HMX, CL-20 and PETN) were investigated and compared to that of TKX-50 [56]. Thermogravimetric analysis (TGA) measurements, using three different kinetic models (Ozawa-Flynn-Wall, ASTM E698 and Friedman) method were evaluated regarding their fit to the experimental data. To evaluate the samples with the NETZSCH Kinetics Neo software [57], thermal gravimetric analysis (TGA) measurements with a PerkinElmer TGA4000 were performed. In order to provide a consistent set of measurements, the samples were dried and sieved to keep them solvent free and within a uniform range of particle size. The measurements were performed at heating rates of 1 K min 1 (m = 2.071 mg), 2 K min 1 (m = 1.879 mg), 5 K min 1 (m = 2.285 mg) and 10 K min 1 (m = 2.105 mg) within a temperature range of 303 K to 673 K.

Using the Friedman method, the long-term stabilities for RDX, HMX, CL-20, PETN and TKX-50 could be predicted for each compound over 10 years (Fig. 16) [56]. In order to investigate the effect of different climate conditions on the stability of TKX-50 in storage scenarios, calculations were performed using climatic data for specific cities averaged over the past 30 years. In summary, the highest long-term stability can be predicted for CL-20 and the lowest for PETN (Fig 17). TKX-50 shows excellent longevity, with a slightly better behavior than RDX.

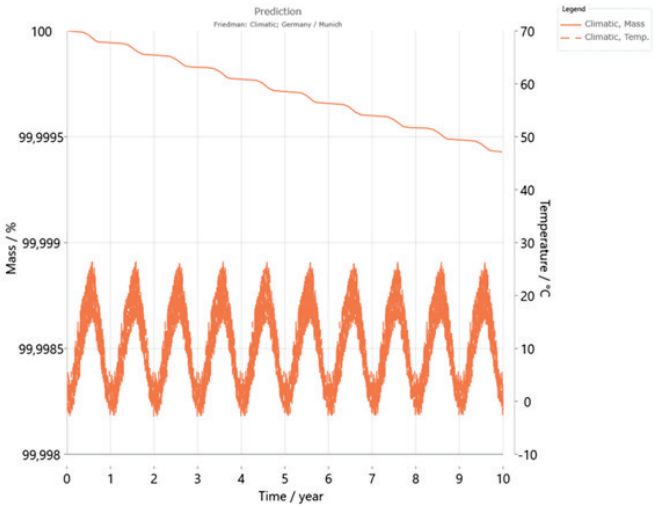

Fig. 16. Climatic prediction of TKX-50 for 10 years using the climate zone Munich [56].

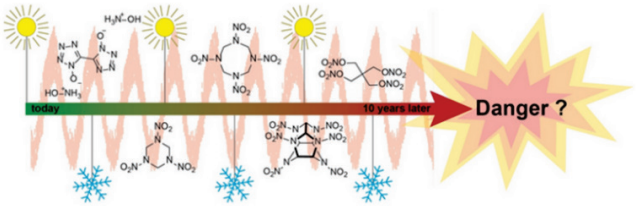

Fig. 17. Thermal aging behavior of different explosives [56].

In order to validate the calculated results, the five compounds were stored at 100°C for 4 weeks and their mass loss was investigated during this time. The obtained data was consistent to the kinetic predictions (Fig. 18).

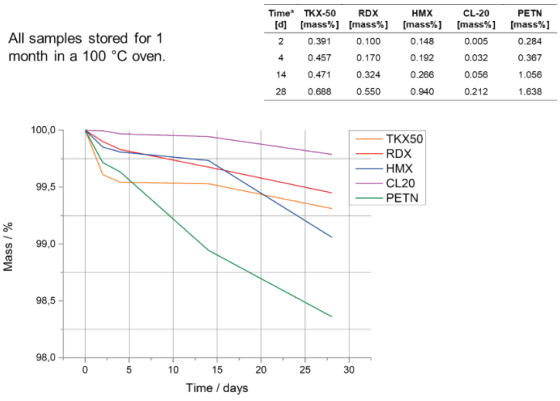

Fig. 18. Mass loss of common explosives at 100°C, over a four-week timespan [56].

In the introduction section it was stated that the environmental impact of energetic materials is one aspect which must be considered seriously for any new compound which aims to proceed to large-scale production. The REACH conform synthesis of TKX-50 shown in Fig. 7 is highly important in this context. Increasingly, the toxicity of the energetic material itself or the compounds used or produced in its synthesis, as well as its detonation products is a factor which is decisive in determining whether an

energetic compound has potential for real-life application. Tests performed on TKX-50 showed no signs of cytotoxicity for TKX-50. Furthermore, the results of mutagenic potential investigations also indicated that TKX-50 and its metabolites have no mutagenic effects on all tested strains of S. typhimurium and E. [58].

3. Oxidizers

In contrast to nitrogen-rich secondary explosives which have high percentage nitrogen contents, for oxidizers, a high percentage oxygen content is the goal. The synthesis of new oxidizers containing only the elements C, H, N, O is a challenging area, since the presence of each C atom and two H atoms requires two oxygen atoms in order to achieve an oxygen balance of zero with respect to CO. By far, the most widely used and standard oxidizer for all large-scale applications is ammonium perchlorate, NH_4+ClO_4- (AP). While AP has many properties that make it an excellent oxidizer, it unfortunately contains chlorine, which forms environmentally problematic HCl on combustion and in addition, perchlorate is of environmental concern. Therefore, there is considerable effort being made around the world to synthesize halogen-free oxidizers, with the goal of replacing the currently-used AP. Arguably, the synthesis and development of halogen-free green oxidizers is one of the areas of energetic materials which has made perhaps slower progress due to the challenges involved. Oxidizers which do not contain halogens, but which have properties equal to those of ammonium perchlorate have been a target for a long time. However, ammonium perchlorate (AP) has never been matched (Tab. 6). The values for AP are compared with those for the compound tris(2,2,2-trinitroethyl)orthoformate (which is commonly referred to in the energetic material literature as either 2,2,2-trinitroethyl formate or TNEF) in table 6.

Table 6. TNEF and AP main properties [28], [29], [30].

	TNEF	**AP**
Molecular formula	$C_7H_7N_9O_{21}$	NH_4ClO_4
Molecular mass [g mol^{-1}]	553.2	117.49
N [%]	22.8	11.92
$\Omega(CO_2)$ [%]	+10.1	+27.2
Heat of formation	−1,021 kJ kg^{-1}	−2,515kJ kg^{-1}

New oxidizers are a synthetic challenge, and the incorporation of larger quantities of oxygen into C,H,N,O generally requires the following aspects to be taken into account. First of all, it is difficult to synthesize C/H/N/O compounds with a positive oxygen balance since C and H require O atoms following the Springall-Roberts rules to form CO (or CO_2) and H_2O during combustion. This is especially true when considering the oxygen balance with respect to CO_2 (ΩCO_2), since in this case every C atom in the molecule requires 2 x O atoms (formation of CO_2) and every two H atoms require 1 x O atom (formation of H_2O) in order to reach ΩCO_2 = 0. Consequently, this means that every –CH_2 group present requires more than 3 x O atoms to have a positive ΩCO_2 value, meaning that, for example, pro -CH_2 group, 11/2 -NO_2 groups must be present. However, simply trying to overload a molecule with nitro groups is also problematic, since incorporating large numbers of nitro groups, especially –$C(NO_2)_3$ groups into a molecule risks lowering the thermal stability to a useless level ($T_{dec.}$ < 150°C). Secondly, although a highly positive oxygen balance is obviously on paper good for an oxidizer, it has been observed from testing oxidizers that higher oxygen balances generally result in higher impact sensitivities. An oxidizer which is highly impact sensitive would also not be useful for most large-scale applications.Despite these restrictive issues, progress has been made in halogen-free oxidizers, and out of all of the oxidizers which have been investigated by the energetic materials group at LMU, the best three examples are probably bis(2,2,2-trinitroethyl)oxalate [BTNEO] (1), 2,2,2-trinitroethyl-nitrocarbamate [TNENC] (2) and 2,2,2-trinitroethyl formate [TNEF] (3) (more correctly referred to as tris(2,2,2-trinitroethyl)orthoformate) (Fig. 19) ([59], [60], [61], [62], [63], [64]).

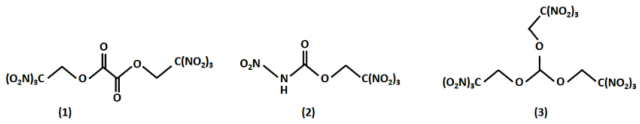

Fig. 19. New halogen-free CHNO oxidizers.

There are some aspects which are common to all three of these halogen-free oxidizers. In all three compounds no halogen is present, all are neutral molecules (AP is a salt), oxygen-rich -$C(NO_2)_3$ groups are present and O atoms have also been incorporated into the carbon skeleton to assist in achieving as positive an oxygen balance as possible. All three compounds possess a positive oxygen balance with respect to CO and CO_2 and have acceptable sensitivity parameters (Tab. 7). Unfortunately, the decomposition temperature of the nitrocarbamate (**2**) is only 153°C which is too low for application. This leaves the oxalate (**1**) and the formate (**3**) as the more promising candidates. The highly positive oxygen balance of 30.4% (with respect to CO), high density of 1.81 g cm^{-3} and a decomposition temperature of 192°C makes overall 2,2,2-trinitroethyl formate [TNEF] (**3**) the best candidate compound out of the three shown in Fig. 19. In addition, it should be mentioned that the sensitivity data of TNEF (IS = 5 J, FS = 9 N, ESD = 0.2 J) are within acceptable ranges. Therefore, TNEF was investigated further, and has already been scaled up in the lab to 100 g scale [65].

Tab. 7. Relevant data for the three oxidizers BTNEO (**1**), TNENC (**2**) and TNEF (**3**) ([28], [29], [30]

	BTNEO (1)	TNENC (2)	TNEF (3)
Formula	$C_6H_4N_6O_{16}$	$C_3H_3N_5O_{10}$	$C_7H_7N_9O_{21}$
M / g mol^{-1}	416	269	553
IS / J	10	10	5
FS / N	> 360	96	9
ESD / J	0.7	0.1	0.2
Ω(CO)/%	15.4	32.7	30.4
$\Omega(CO_2)$/%	7.7	14.9	10.1
m.p. / °C	115	109	128
T_{dec} / °C	186	153	192
ρ / g cm^{-3}	1.84	1.73	1.81
$\Delta H°_f$/kJmol^{-1}	-688	-366	-519

One aspect of oxidizers which is of particular interest currently is their use in thermobaric formulations. Recently, the suitability of TNEF (**3**) to replace ammonium perchlorate (AP) in thermobaric (TBX) formulations has been investigated computationally and experimentally. The thermobaric formulation which was chosen to be investigated consisted of the secondary explosive HMX, Al, binder and TNEF (*tris*(2,2,2-trinitroethyl) orthoformate) (TBX-2). In addition, the analogous formulation was made in which TNEF was replaced by the standard oxidizer AP (TBX-1), and the properties of the two formulations were compared. The formulations each consisted to 40% secondary explosive, 20% Al fuel, 20% binder and 20% of the oxidizer. The detonation velocity of the two thermobaric mixtures was both measured experimentally and calculated, and showed that the VoD of the mixture containing TNEF was essentially identical to that containing AP. Generally, both TBX-formulations showed similar energetic performance, with the formulation containing the halogen-free TNEF (TBX-2) having a slightly higher heat of detonation (Q_{ex}) and detonation temperature (T_{ex}), both of which are advantageous (Tab. 8, Fig. 20).

Table 8. Calculated energetic performance parameters (EXPLO5_V6.05.02) [1] of two TBX formulations (40% secondary explosive, 20% Al, 20% binder, 20% oxidizer) which vary only in the oxidizer used: oxidizer = AP (TBX-1), TNEF (TBX-2) [66].

	TBX-1	TBX-2
Oxidizer present	AP	TNEF
VoD / m s^{-1}	6699	6593
p_{C-J} / GPa	18.2	17.6
$-Q_{ex}$ / kJ kg	8202	8355
T_{ex} / K	4371	4451

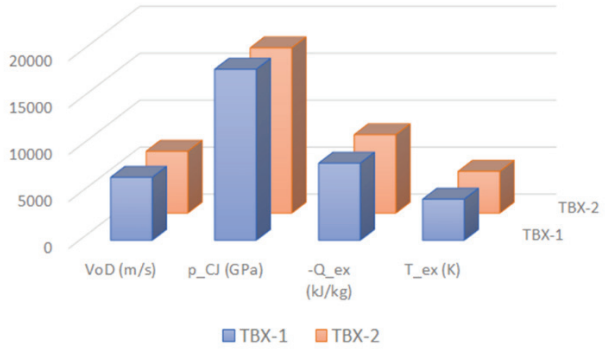

Fig. 20. Graphical representation of the performance parameters of formulation TBX-1 (containing the halogen-containing oxidizer AP) and TBX-2 (containing the halogen-free oxidizer TNEF).

Shock waves generated by the detonation of thermobaric weapons have a much longer duration than those which are generated by conventional high explosives. In addition, they also show a larger lethal radius. Under confinement, thermobaric detonations cause a series of reflected shock waves which maintain the fireball, and can extend its duration to between 10 and 50 ms, as exothermic recombination reactions occur. Due to its importance in the area of thermobaric formulations, the maximum overpressures generated from 600 g each of the formulations TBX-1 and TBX-2 were both calculated and experimentally measured as a function of the measuring spot distance from the center of the detonation (Fig. 21).

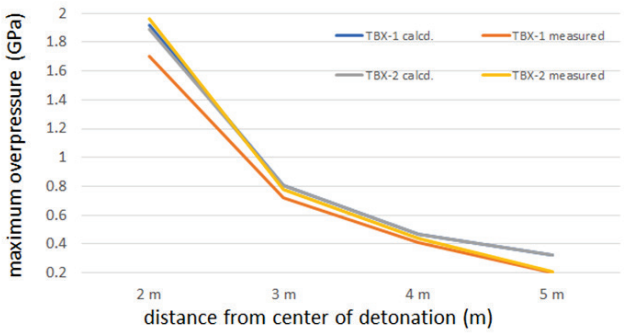

Fig. 21. The maximum overpressures generated from 600 g each of the formulations TBX-1 and TBX-2 as a function of the distance from the center of detonation.

Currently, the properties and performance of the TBX (TBX-2) containing the new, halogen-free oxidizer TNEF in the formulation are essentially as good as the same TBX formulation in which AP is present in the formulation (TBX-1) instead of TNEF. The advantage of using AP in the formulation is its cost, availability and the huge amount of information which is already known about many of the properties of AP. The disadvantage of using AP is that it contains chlorine, which forms HCl, which is problematic in terms of the environment, and contains the perchlorate ion which is problematic in terms of its effects on human health. Although in the early stages of development, using TNEF would eliminate both of these problems. However, much more work must be invested into TNEF before its potential for application can be reliably established.

4. Conclusion

An overview of the best secondary explosive (TKX-50) and oxidizer (TNEF) which have been developed in the energetic materials group at LMU shows has been given. The investigations and properties which have been discussed illustrate that extensive investigations must be performed before a compound can be truly classified as a candidate compound for potential future applications. While in the first instance several compounds may show good sensitivity to impact and friction and high calculated detonation velocities, this alone is not enough to categorize a compound as being a potential replacement for the currently-used HMX or RDX. TKX-50 act as an excellent illustrative example of the considerable factors which must be established for any energetic compound prior to its selection for up-scaling. In addition to considering the properties of pure TKX-50, extensive investigations have also been described into the suitability of TKX-50 for use as a secondary explosive in composite explosives and also in thermobaric formulations. The initial results from these investigations are highly promising. The difficulties in preparing new, halogen-free oxidizers with suitable properties are not identical with those

for developing new secondary explosives. The specific issues relevant to the development of new, environmentally more compatible oxidizers has been illustrated using the compounds BTNEO, TNENC and TNEF. Although TNENC has an excellent oxygen balance (which is essential for an oxidizer), unfortunately the decomposition temperature of TNENC is too low to make it of interest for further consideration. The safety, reliability and longevity of an oxidizer are essential properties. The oxidizer TNEF shows a particularly good combination of properties, and has therefore been increased to a 100 g scale for further investigation. The use of TNEF in a thermobaric formulation recently showed good performance and currently TNEF remains a promising candidate for use as an oxidizer in the future.

Acknowledgments
The author is indebted to and thanks the friends and colleagues listed below for their year-long, great and stimulating collaboration: Dr. Jasmin T. Lechner (LMU Munich & ICT Karlsruhe), Prof. Dr. Stanislaw Cudzilo (WAT Warsaw), Dr. Danica Bajic (Military Technical Institute, Belgrade), Prof. Dr. Muhamed Suceska (Zagreb University) and Dr. Vladimir Golubev (LMU Munich).

5. References

[1] Suceska, M., "EXPLO5, version V6.06.01", Zagreb (2021).
[2] Agrawal, J. P.; Hodgson, R. D. (2007) Organic Chemistry of Explosives, Weinheim: Wiley-VCH, 2007.
[3] Agrawal, J. P. (2010) High Energy Materials. Weinheim: Wiley-VCH, 2010
[4] Brinck, T. (Ed.) (2014) Green Energetic Materials, Weinheim: Wiley 2014.
[5] Fair, H. D.; Walker, R. F. (1977) Energetic Materials, Vol. 1 & 2, New York: Plenum Press, 1977
[6] Fordham, S. (1980) High Explosives and Propellants, 2nd edn., Oxford: Pergamon Press, 1980
[7] Keshavarz, M.H., Klapötke, T.M. (2018) The Properties of Energetic Materials. Berlin, Boston: de Gruyter, 2018
[8] Keshavarz, M.H., Klapötke, T.M. (2020) Energetic Compounds, 2nd edn.; Berlin, Boston: de Gruyter, 2020
[9] Koch, E.C. (2019) Sprengstoffe, Treibmittel, Pyrotechnika, 2. Aufl.. Berlin, Boston: de Gruyter, 2019
[10] Köhler, J., Meyer, R., Homburg, A. (2008) Explosivstoffe, 10. Aufl.. Weinheim: Wiley-VCH, 2008
[11] Klapötke, T.M. (2025) Chemistry of High Energy Materials, 7th edn. Berlin, Boston: Walter de Gruyter, 2025
[12] Lai, Q., Long. Y., Yin, P., Shreeve, J.M., Pang, S. (2024). „Thinking Outside the Energetic Box: Stabilizing and Greening High-Energy Materials with Reticular Chemistry", Acc. Chem. Res., (57): 2790-2803.
[13] Olah, G.A.; Squire, D.R. (1991) Chemistry of Energetic Materials. San Diego: Academic Press, 1991
[14] Urbanski, T., (1964/1984) Chemistry and Technology of Explosives, Vol. 1–4. Oxford: Pergamon Press, 1964/1984
[15] Venugopalan, S., Demystifying Explosives: Concepts in High Energy Materials, Elsevier, Amsterdam, (2015).
[16] Gao, H., Shreeve, J.M. (2011). "Azole-Based Energetic Salts", Chem. Revs., (111): 7377-7436
[17] Klapötke, T.M. (2007) "New Nitrogen-Rich High Explosives", in: Klapötke, T.M. (vol. editor), Mingos, D.M.P. (series editor) Structure and Bonding, Vol. 125/2007: High Energy Density Compounds. Berlin, Heidelberg: Springer.
[18] Klapötke, T.M., Chapman, R.D. (2016) "Progress in the Area of High Energy Density Materials", in Mingos, D.M.P. (Ed.) 50 Years of Structure and Bonding – The Anniversary Volume, Structure and Bonding 172, Cham, Switzerland: Springer, pp. 49–64.
[19] Liu, Y., Zhang, X., Li, J., Pei, X., Pang, S., He, C. (2025). "Construction of Bis-Heterocyclic Energetic Compounds via C-N Coupling Reactions", JACS Au, (5): 990-997
[20] O'Sullivan, O.T., Zdilla, M.J. (2020). "Properties and Promise of Catenated Nitrogen Systems as High-Energy-Density Materials", Chem. Revs., (120): 5682-5744.
[21] Yount, J., Piercey, D.G. (2022). "Electrochemical Synthesis of High-Nitrogen Materials and Energetic Materials", Chem. Revs., (122): 8809-8840
[22] Fischer, N., Fischer, D., Klapötke, T.M., Piercey, D.G., Stierstorfer, J. (2012). „How High Can You Go? Pushing the Limits of Explosive Performance", J. Mater. Chem., (22): 20418-20422
[23] Klapötke, T.M., Fischer, N., Fischer, D., Piercey, D.G., Stierstorfer, J., Reymann, M. (2013a). "Energetic active composition comprising a dihydroxylammonium salt or diammonium salt of a bistetrazolediol". Ger. Offen., DE 102011081254 A120130221.
[24] Klapötke, T.M., Fischer, N., Fischer, D., Piercey, D.G., Stierstorfer, J., Reymann, M. (2013b). "Energetic active composition comprising a dihydroxylammonium salt or diammonium salt of a bistetrazolediol". PCT Int. Appl., WO 2013026768 A1 20130228.
[25] Klapötke, T.M. (2020). „Ein neuer Sekundär-Sprengstoff: TKX-50", Chemie in unserer Zeit, (54): 234–241
[26] Silva, A.L.R., Almeida, A.R.R.P., Ribeiro da Silva, M.D.M.C., Reinhardt, J., Klapötke, T.M. (2023). "On the Enthalpy of Formation and Enthalpy of Sublimation of Dihydroxylammonium 5,5′-bitetrazole-1,1′-dioxide (TKX-50)", Prop. Explos. Pyrotech., (48): e202200361
[27] Delage, A., Eck, G., Alaime, T., Lacemon, F., Klapoetke, T.M., Stierstorfer, J., Boelter, M. "Process for sequential one-pot synthesis of TKX-50 for energetic compositions". World Intellectual Property Organization, WO2022129724 A1 2022-06-23 and FR3118034 A1 2022-06-24.
[28] Klapötke, T.M. (2021) Energetic Materials Encyclopedia, 2th Edition. Berlin, Boston: de Gruyter,

2021
[29] Klapötke, T.M. (2021) “TKX-50: A highly promising secondary explosive” in Trache, D., Benaliouche, F., Mekki, A. (Eds.) Materials Research and Applications (Select Papers from JCH8-2019). Singapore: Springer.
[30] Klapötke, T.M., Suceska, M. (2021). “Theoretical evaluation of TKX-50 as an ingredient in rocket propellants”, Z. Anorg. Allg. Chem., (647): 572-574
[31] Yu, Y., Chen, S., Li, X., Zhu, J., Liang, H., Zhang, X., Shu, Q. (2016). “Molecular Dynamics Simulations for 5,5’-Bistetrazole-1,1’-diolate (TKX-50) and its PBXs”, RSC Adv., (6): 20034-20041.
[32] Yu, Y., Chen, S., Li, T., Jin, S., Zhang, G., Chen, M., Li, L. (2017). “Study on a Novel High Energetic and Insensitive Munitions Formulation: TKX-50 Based Melt Cast High Explosive”, RSC Adv., (7): 31485-31492
[33] Liu, D., Chen, J., Yang, R., Xiao, L., Zhang, G., Feng, X., Zhang, K., Jiang, W., Hao, G. (2024). “An Overview on Synthesis, Explosion, Catalysis, Modification, and Application of Dihydroxylammonium 5,5’-Bistetratzole-1,1’-diolate (TKX-50)”, Chem. Mater., (36):) 3496-3535.
[34] Graswald, M., Feller, M., Komanschek, V. TDW Gesellschaft für Verteidigungstechnische Wirksysteme, DE102019008980.
[35] Anniyappan, M., Talawar, M.B., Sinha, R.K., Murthy, K.P.S. (2020). “Review on Advanced Energetic Materials for Insensitive Munition Formulations”, Combust, Explos., Shock Waves, (56): 495-519
[36] Herrmann, M., Förter-Barth, U. (2021). “Thermal Behavior and Micro Structure of TKX-50”, Prop. Expl. Pyrotech., (26): 262-266.
[37] Golubev, V.K., Klapötke, T.M. (2022). “Calculated estimations of the performance for TKX-50 based formulations”, NMH 2021 Proceedings, J. Phys.: Conference Series (JPCS) (2154): 012006.
[38] Klapötke, T.M. (2023) “New High Explosives and Melt Casts in the Western World (excl. China)”, in Pang, W., DeLuca, L. (Eds.) Nano- and Micro-scale Energetic Materials, Propellants and Explosives. Weinheim: Wiley, pp. 455–498.
[39] Sabatini, J.J., Oyler, K.D. (2016). “Recent Advances in the Synthesis of High Explosive Materials”, Crystals, (6): 5
[40] Muravyev, N.V., Fershtat, L., Zhang, Q. (2024). “Synthesis, Design and Development of Energetic Materials: Quo Vadis?”, Chem. Eng. J., (486): 150410
[41] Pang, W.Q., Klapötke, T.M., DeLuca, L.T., Wang, K., Qin, Z., Hu, Y. (2023) “Effect of TKX-50 on the performance of solid propellants and explosives: a review”, in Pang, W., DeLuca, L. (Eds.) Nano- and Micro-scale Energetic Materials, Propellants and Explosives. Weinheim: Wiley, pp. 149–190.
[42] Zhang, M., An, T., Song, X., Zhao, F., Yao, E., Xue, Y., Wang, Y., Chen, X., Yuan, Z., Ciao, L. (2024). “Exploration of TKX-50-M (M = Pb, Bi and Cu) as Insensitive High-Energy Combustion Catalysts of HMX-CMDB Propellant”, Chem. Eng. J., (497): 154982
[43] Pang, W.Q., DeLuca, L.T., (2015). “Effects of TKX-50 on the Properties of HTPB-Based Composite Solid Propellant”, 7th European Conf. for Aeronautics and Space Sciences (EUCASS) (2015). DOI:10.13009/EUCASS2017-544
[44] Klapötke, T.M., Cudziło, S., Trzciński, W.A., Paszula, J., Bauer, L., Riedelsheimer, C., Lechner, J. (2023). “Performance of TKX-50 in Thermobaric Explosives”, Prop. Explos. Pyrotech., (48): e202300010
[45] Klapötke, T.M., Cudziło, S., Trzciński, W.A. (2022). “An Answer to the Question about the Energetic Performance of TKX-50”, Prop. Explos. Pyrotech., (47): e202100358.
[46] Sinditskii, V.P., Filatov, S.A., Kolesov, V.I., Kapranov, K.O., Asachenko, A.F., Nechaev, M.S., Lunin, V.V., Shishov, N.I. (2015). „Combustion behavior and physico-chemical properties of dihydroxylammonium 5,5′-bistetrazole-1,1′-diolate(TKX-50)“, Thermochim. Acta, (614): 85–92
[47] Paraskos, A., „Tracking Sensitive Intermediates by In Situ FTIR for the Safe Synthesis of Energetic Materials“, at: METTLER TOLEDO R&D and Process Development in the Pharmaceutical and Chemical Industries Seminar, The Hyatt New Brunswick, NJ, June 9th (2016).
[48] Schaller, U., Personal communication, Institute of Chemical Technology (ICT), Pfinztal, Germany (2020).
[49] Gottfried, J.L., (2014) “New Laboratory-Scale Method for the Determination of Explosive Performance from Laser-Induced Shock Waves”, ARL-TR-6844, Army Research Laboratory, Aberdeen Proving Ground, MD, USA
[50] Gottfried, J.L., (2015). “Laboratory-Scale Method for Estimating Explosive Performance from Laser-Induced Shock Waves”, Prop. Explos. Pyrotech., (40): 674–681
[51] Gottfried, J.L., Klapötke, T.M., Witkowski, T.G. (2017). “Estimated Detonation Velocities for TKX-50, MAD-X1, BDNAPM, BTNPM, TKX-55, and DAAF using Laser-induced Air Shock from Energetic Materials Technique”, Prop. Explos. Pyrotech., (42): 353–359
[52] Gottfried, J.L., Wainwright, E.R. (2025). “Laser-Induced Air Shock From Energetic Materials (LASEM): A Novel Microscale Technique for Characterizing Energy Release at High Heating Rates”, J. Energet. Mater., (43): 1-61
[53] Fischer, D., Gottfried, J.L., Klapötke, T.M., Karaghiosoff, K., Stierstorfer, J., Witkowski, T.G. (2016). “Synthesis and Investigation of Advanced Energetic Materials Based on Bispyrazolylmethanes”, Angew. Chem. Int. Ed., (55): 16132–16135; Angew. Chem., (128): 16366–16369.
[54] Bauer, L., Benz, M., Klapötke, T.M. (2022). “Linear Correlation Between Quantity of Confined Explosive and Bulge of an Underlying Aluminum Block Using the SSRT Setup”, Prop. Explos. Pyrotech., (47): e202100332
[55] Bauer, L., Benz, M., Klapötke, T.M., Selmeier, A. (2022). “Evaluation of SSRT-Test by Classical Gravimetric Analysis and Optical Topographic Measurement: A Comparative Study”, Prop. Explos. Pyrotech., (47): e202200113

[56] Harter, A., Klapötke, T.M., Lechner, J., Stierstorfer, J. (2022). “Kinetic predictions concerning the long-term stability of TKX-50 and other common explosives using the NETZSCH Kinetics Neo software”, Prop. Explos. Pyrotech., (47): e202200031
[57] NETZSCH Kinetics Neo software, version 2.5.0.1, (2021)
[58] Klapötke, T.M., Scharf, R., Stierstorfer, J. (2014). “Aquatic toxicity determination of energetic materials using the luminescent bacteria inhibition test”, New Trends in Research of Energetic Materials, University of Pardubice, Czech Republic, p. 542
[59] Trache, D., Klapötke, T.M., Maiz, L., Abd-Elghany, M., DeLuca, L.T. (2017). “Recent Advances in New Oxidizers for Solid Rocket Propulsion”, Green Chem., (19): 4711–4736.
[60] Frankel, M.B. (1962). “Polynitro Carbamates and N-Nitrocarbamates”, J. Chem. Eng. Data, (7): 410
[61] Klapötke, T.M., Krumm, B., Moll, R., Rest, S.F. (2011). “CHNO Based Molecules Containing 2,2,2-Trinitroethoxy Moieties as Possible High Energy Dense Oxidizers”, Z. Anorg. Allg. Chem., (637): 2103-2110
[62] Hill, M.E., Shipp, K.G. (1970). Process for acetal preparation. US Patent US3526667
[63] Sheremetev, A.B., Yudin, I.L. (2005). “Synthesis of 2-R-2,2-dinitroethanol orthoesters in ionic liquids”, Mendeleev Commun., (15): 204–205
[64] Shipp, K.G., Hill, M.E. (1966). “Acetal preparation in sulfuric acid”, J. Org. Chem., (31): 853–856
[65] Dosch, D.E., Andrade, K., Klapötke, T.M., Krumm, B. (2021). “An Optimized & Scaled-up Synthetic Procedure for Trinitroethyl Formate TNEF”, Prop. Explos. Pyrotech., (46): 895-898
[66] Klapötke, T.M. (2024). “New Secondary Explosives and Oxidizers Developed at LMU”, 53rd Intl. Annual Conf., ICT, Karlsruhe; June 25th–28th , V1

Dobrilović Ivana[1], Dobrilović Mario[1], Sućeska Muhamed[1], Kovačević - Zelić Biljana[1], Stanković Siniša[1]

Modeling of soil density zones in the vicinity of an explosive charge

[1] University of Zagreb, Faculty of Mining, Geology, and Petroleum Engineering, Pierottijeva 6, 10000 Zagreb

Abstract

Modeling the change in the parameters of the soil exposed to the performance of the explosion, considering the heterogeneity of the soil, the dependence on the water content and the different calibration experimental parameters, is a challenge. The models, incorporated in the computer program Ansys 2020 R1 Autodyn 2D hydrocode, were used to model the performance of the explosive charge in the soil and can be used with certain accuracy to estimate the change in soil density in the environment of the explosive charge in an infinite environment. The processes of performance of three types of explosives on the density of the soil in the vicinity of the explosive charge and the influence of the mass of the ANFO explosive charge on the radius of the resulting expansion were modeled. The modeling results for cavity diameter are compared with the experimental data and presented in the article.

***Keywords**: soil, density zone, explosive charge, Autodyn 2D hydrocode*

1. Introduction

The energy of the explosion is used for various purposes in the military and civilian fields. Blasting is a technique of using explosives primarily for crushing solid rocks, in mining and construction applications. Blasting in the soil can be classified as special methods that include excavation, drainage, soil improvement and the creation of expansion for the placement of anchors. Modeling the change in the parameters of the soil exposed to the performance of the explosion, considering the heterogeneity of the soil, the dependence on the water content and the different calibration experimental parameters, is a challenge. The models, incorporated in the computer program Ansys 2020 R1 Autodyn 2D hydrocode, were used to model the performance of the explosive charge in the soil and can be used with certain accuracy to estimate the change in soil density in the environment of the explosive charge in an infinite environment. The processes of performance of three types of explosives on the density of the soil in the vicinity of the explosive charge and the influence of the mass of the ANFO explosive charge on the radius of the resulting expansion were modeled. Modeled expansion dimensions were compared with experimental data.

The soil is a three-phase system (solid particles, water and air) and it is difficult to predict soil deformation under impact load such as one that is produced by an explosion. Difficulty is in the main fact that effective stress principle and soil dynamics principles are invalid under blast loading. The solid particles deform under loading, and water and air are trapped in the voids because of the very short load duration, thus providing additional load resistance [1]. The common practice in modeling soil behavior under a blast load is primarily based on empirical formulas from field tests [1]. According to the complexity of the problem, soil behavior under blast loading has been studied by many researchers: Wang and Lu 2003; Tong and Tuan 2007; Grujicic et al. 2008 and the others [2]. An additional difference appears if the soil is cohesive or non-cohesive. In cohesive soils, two deformation mechanisms exist. The first deformation mechanism, at low pressure, the soil skeleton deformation is determined by the elastic deformation of bonds on the contact surfaces of grains; the first mechanism at high pressure is determined by a failure in bonding and the displacement of grains (plastic deformation). The second deformation mechanism is the deformation of all the soil phases. When soil is being compressed, both mechanisms act simultaneously, but at certain phases of the loading, one of the mechanisms predominates [3]. Commercial explosives used for blasting are characterized by non-ideal detonation (lower energy, pressure and velocity of detonation and longer time of heat release [4, 5, 6].

ANFO explosives, AN powder explosives and water gels are commercial explosives. They show the non-ideality of detonation to a certain extent, in the sense of deviation from the classic, hydrodynamic detonation model. At the same time, the pressure and velocity of the detonation are significantly dependent on the conditions in which the process takes place, that is, the confinement of the system boundaries and the stiffness of the boundaries (for example, in the case of detonation in air, water, rock or a steel pipe); the diameter and size of the charge and the energy and speed of the initial impulse. Related to the above, when modeling the process of expansion in clay and densification of clay in the vicinity of the explosive charge, it is necessary to rationally choose the parameters that describe, in the case of the application of Autodyne hydrocode, JWL (Jones Wilkins Lee) the adiabatic of the detonation product gases in accordance with the shape and mass of the explosive charge and the conditions in which the process takes place. Since the models or codes for the calculation of detonation parameters (detonation velocity, detonation pressure, explosion energy, volume of gases produced by detonation) are found on several calculation approaches based on the chemical composition of the explosive and the ideal detonation process, it is necessary to make corrections based on the measured detonation velocities. Thus, when modeling with Ansys 2020 R1 Autodyn 2D hydrocode, correction of JWL parameters obtained by computer code Explo 5 with values of detonation velocities measured on the same sample size in simulated conditions of clay soil was made for the explosive input data. The specified explosives (ANFO, ammonium nitrate powder and water gels) used in the

research differ in their performance, which can be expressed by the parameters given in table 1. The performance of explosives is expressed in relative values obtained by dedicated testing methods and reflects the ability of the explosive to function in certain conditions or media. The working performance is determined mostly by the detonation velocity and detonation pressure of the explosive used. The results of recent research have shown that the primary role in the performance of explosives in the soil [7] is played by the amount of energy applied, i.e. the mass of the explosive, and only secondarily by the type of explosive, i.e. the velocity and pressure of detonation. During the detonation process of the explosive, by rapid oxidation, it turns into highly compressed gaseous products (pressures are from several tens to several

hundreds of kBar). During adiabatic, almost instantaneous expansion, the gases have an impact effect on the surrounding soil and, after the soil shifts in the immediate vicinity of the blasthole, they generate an area of soil with higher densities. The highest densities occur at the boundary of the expansion and decrease with distance from the blasthole. Such a distribution is a consequence of the consumption of impact energy, i.e. the loss of gas pressure. According to previous results, the volume of the resulting expansion depends mostly on the mass of the explosive, while the values of soil densities can be related to the type of explosive, i.e. the magnitude of individual detonation pressures. The paper analyzes the behavior of soil during shock wave propagation, through density changes in cohesive soil. Laboratory and field tests were conducted as part of previous research. Laboratory tests included determining the physical and mechanical parameters of the soil, while field tests included measuring the geometric parameters of the expansion caused by blasting with ANFO explosives. Using numerical simulation Ansys 2020 R1 Autodyn 2D hydrocode for different ANFO charge masses, the expansion dimensions and soil densities in the vicinity of the expansion were determined. After validating the model solution with experimental values, simulations were conducted for two more types of commercial explosives, namely AN powder and water-gel explosives. In this part of the research, an analysis of density changes in the surrounding soil after blasting was conducted and the soil response zones to the passage of a shock wave caused by the detonation of an equal mass of 1 kg of different commercial explosives were defined.

2. Materials and Methods

2.1. Soil characteristics

Detailed laboratory analyzes of the soil in which the blasting was carried out showed that it is highly plastic clay (content: 3.5% gravel, 3.1% sand, 55.6% silt and 37.8% clay) [7]. Laboratory analysis of soil compressibility in an oedometer were carried out and the results are shown in Figure 1 in the form of a Hugoniot diagram.

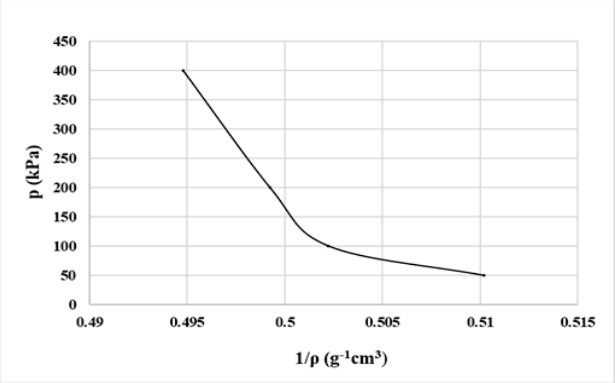

Fig. 1. Hugoniot curve for tested soil

The initial soil density was determined, as 1.96 g/cm^3, and the density of solid particles as 2.71 g/cm^3.

2.2. Explosive characteristics

Commercial explosives used in the research differ in composition and type of mixture and thus in detonation

characteristics. The basic, relevant parameters of the explosives used are shown in Table 1.

Table 1. Explosive parameters

Type of explosive	Chemical composition	Density (g/cm^3)	Velocity of Detonation (Measured) (m/s)	Pressure [GPa]	Theoretical Heat of Detonation (Literature and Producer Declaration) (KJ/kg)
ANFO	NH_4NO_3 and mineral oil	0.90	2000	0.86	3597
Ammonium nitrate powder explosive	ammonium nitrate, trinitrotoluene, dinitrotoulene, paraffin wax, and moisture	1.05	4000	3.24	4276
Watergel	NH_4NO_3, MMAN, water, $NaNO_3$, and aluminum	1.25	4576	5.83	4591

The velocities of detonation (VOD) of the concerned explosive properties were derived from experimental results, measured by the electro-optical method, with the same properties and confinement at the test field in charges as in simulations. The measured values deviate from the declared, theoretical values of the detonation velocity, especially with ANFO explosive due to the pronounced non-ideality, especially in the form of the applied charge.

2.3. Numerical simulation

Numerical simulation was performed using Autodyne software via Compaction EOS Linear model where the elastic bulk stiffness of the material is defined as a piecewise linear curve of sound speed (c) versus density (ρo). The bulk stiffness of the material is given by equitation:

$$K = \rho_0 c^2 \quad (1)$$

The level of compaction in the material is given by equitation:

$$\alpha = \frac{\rho_s}{\rho_0} \quad (2)$$

Initially, ρ_o will be equal to the value defined in the density property of the material. Material property ρ_s is the solid zero pressure density of the material and corresponds to the fully compacted material density. For a porous material the initial density will be less than the solid density hence the value of α will be greater than 1.0. As compaction takes place, α will reduce to a value of 1.0 for the fully compacted state [8].

The explosive detonation and expansion were modeled by using Jones-Wilkins-Lee (JWL) equation of state (EOS) given by the following equitation:

$$P = C_1\left(1 - \frac{\omega}{R_1 V}\right)e^{-R_1 V} + C_2\left(1 - \frac{\omega}{R_2 V}\right)e^{-R_1 V} + \frac{\omega E}{V} \quad (3)$$

where, P is the hydrostatic pressure, C_1, C_2, R_1, R_2 and ω empirically derived constants which provides different values for different explosives; V is the specific volume of detonation product over the specific volume of undetonated explosive and E is specific internal energy [8]. JWL constants for used explosives are determined using termocode EXPLO 5 and they are given in table 2.

Table 2. JWL coefficients [4].

Type of explosive	A (Mbar)	B (Mbar)	R_1 (-)	R_2 (-)	ω (-)	D (cm/μs)	P (Mbar)	E_0 (Gerg/mm^3)
ANFO	0.062805	0.001513	2.193732	0.464714	0.177879	0.304939	0.01933323	0.029706
Amonnium nitrate powder	0.79023	0.01257	4.6797	0.9529	0.1933	0.4022	0.0379	0.0318
Watergel	2.38931	0.022655	5.203369	1.054384	0.158459	0.4587	0.05828	0.0412

3. Results and discussion

The effect of an explosive charge during detonation in the soil can be visualized through zones that change the surrounding environment through a change in density and a change in particle size and particle bonding. In the blasting of solid rocks, classical models describe a zone of intense crushing in the immediate vicinity of the borehole or charge. In the soil, there is no fracturing, fragmentation and crushing, but rather soil compression and an increase in density, which is determined by the nature of the soil. The outer zone of the explosive performance is a seismic zone in which the density does not change, there is no movement of material and no plastic deformation, but the particles vibrate elastically and dissipate the remaining energy. The sizes of the zones, or their widths seen from the blasthole, depend on the physical and mechanical properties of the soil, the detonation properties of the explosive and the mass of the explosive charge.

By releasing the energy of the explosive through the detonation process, ideal or non-ideal, the detonation gases, which are heated to several thousand degrees and compressed to pressures from several tens of kBar to several hundred kBar in the volume of the initial explosive, suddenly expand. In this case, they act on the environment via a shock wave that initially fractures and/or pushes the material of the environment (depending on the properties and type of the environment). Secondarily, immediately after the impact, the products of the expansion push the material of the environment and either crush it or increase its density in the case of soil. At the end of the process, around the expansion in the soil caused by the performance of the explosive charge, an area of increased soil density is formed with a maximum, crystalline density in a very thin zone directly next to the contact of the expansion and with a distribution of densities to the undisturbed soil density. The simulated processes formed zones of different densities, where the widths of the zones, or the volumes of the substance with a change in density, depend on the mass and type of explosive charge described by the detonation parameters of the explosive used.

The results for all three types of explosives showed that the surrounding soil behaved uniformly with the use of the same mass of explosive. The first zone is a zone of sudden increase in soil density and it extends from the edge of the expansion to 450 mm viewed from the center of the detonation zone. The second zone, or the zone of gradual decrease in density, extends from 450 mm to 600 mm. The third zone extends from 600 mm to 1350 mm, in this zone the density drops to approximately the initial value, while in the fourth zone (zone around 1500 mm) the soil remains undisturbed.

The results of changes in soil density under the performance of explosives of different detonation properties are shown in Table 3 and in Figures 2, 3 and 4, while the zones are shown in Figure 5.

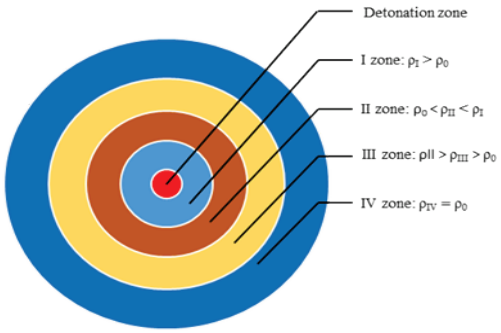

Fig. 2. Density change zones display

Table 3. Results of soil density by zones (1 kg of explosive)

Type of explosive	Zone I Density (g/cm^3)	Zone II Density (g/cm^3)	Zone III Density (g/cm^3)	Zone IV Density (g/cm^3)
ANFO	2.46	2.09	2.04 – 2.01	1.96
Amonnium nitrate Powder	2.16	2.03	2.02 – 1.96	1.96
Watergel	-	2.40	2.07 – 2.01	1.96

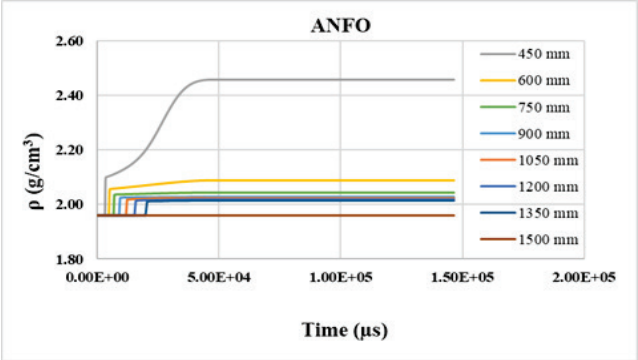

Fig. 3. Density profile of surrounding soil when using ANFO explosive.

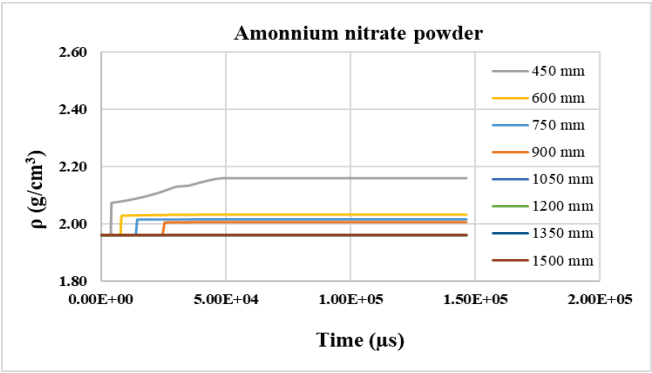

Fig. 4. Density profile of surrounding soil when using ANFO explosive.

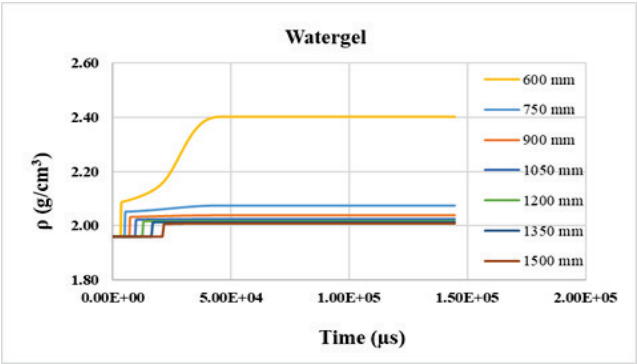

Fig. 5. Density profile of surrounding soil when using Watergel explosive.

The analysis of the results was carried out from the aspect of the size or radius of the resulting expansion and from the aspect of the change in density in the vicinity of the expansion. It can be concluded that 1 kg of commercial explosive of any type (ANFO, Ammonium nitrate powder or Watergel) produces expansions of almost equal dimensions. The simulation results match well with the results of the experiments conducted for ammonium nitrate powder explosive and ANFO explosive. From the experimental data it can be concluded that the sizes of the expansion radii are somewhat larger for ammonium nitrate powder explosive. With a closer comparison and review of the data, such a deviation of approximately ten percent can be attributed to the error in measuring the expansion dimensions during the in situ experiment. The model results were experimentally confirmed for ANFO, while there are no experimental results for ammonium nitrate powder explosives or water gel. Such results can be linked to the fact that the detonation pressures of the product gases, which can be considered the main acting mechanism in the formation of expansion, have values many times

higher than the compressive strengths of the soil. In this case, when acting on the entire volume of soil, due to the significantly higher pressure in relation to the strength, small differences in the pressures of individual explosives do not have a significant impact on the total expansion volume. Analysis of the parameter of the product of the theoretical detonation energy and the volume of the gases produced (QxV), which is called the explosion power, and which can be used to assess the working capacity, results in differences of 15 percent for the observed explosives. It can be concluded that the amount of explosion power is relevant to the size of the expansion in the soil. For the observed explosives, the explosion powers range from 2000 to 2200, i.e. they differ within 15%. The results of the modeled and measured explosion power expansion radii for the explosives used are given in Table 4.

The results are shown in table 5 and in figures 6, 7, 8 and 9.

Table 5. Explosive parameter

Total mass of ANFO explosive	Zone I Density (g/cm^3)	Zone II Density (g/cm^3)	Zone III Density (g/cm^3)	Zone IV Density (g/cm^3)
0.23 kg	2.08	2.03	2.02 – 1.96	1.96
0.4 kg	2.39	2.06	2.03 – 1.96	1.96
1 kg	2.46	2.09	2.04 – 2.01	1.96
1.5 kg	-	-	2.15 – 2.02	1.96

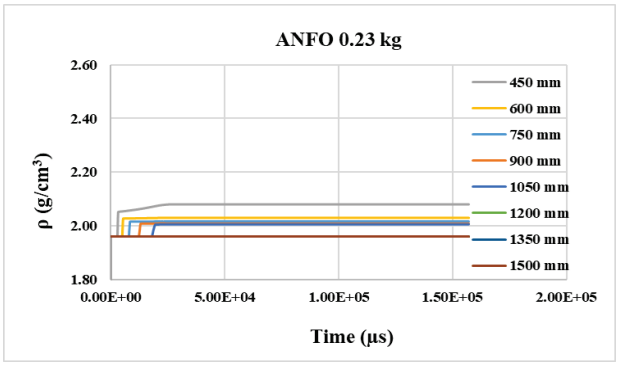

Fig. 6. Density profile of surrounding soil (0.23 kg of ANFO).

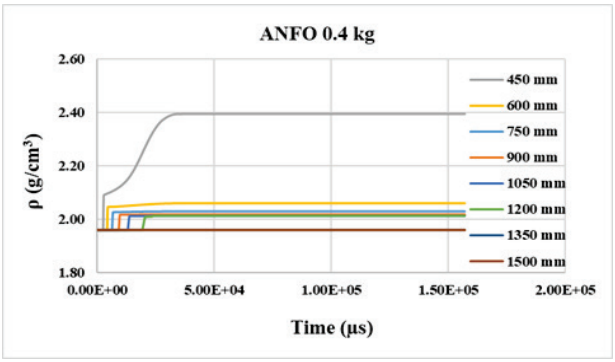

Fig. 7. Density profile of surrounding soil (0.4 kg of ANFO).

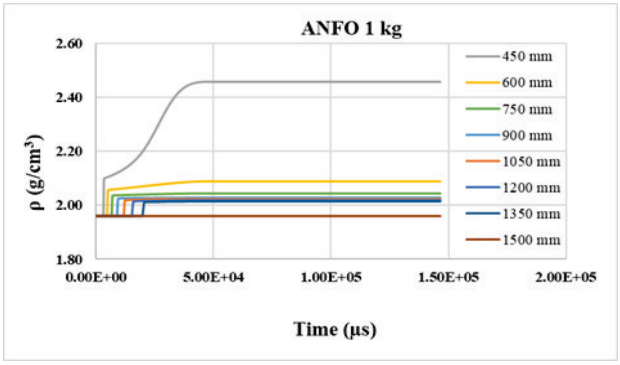

Fig. 8. Density profile of surrounding soil (1 kg of ANFO).

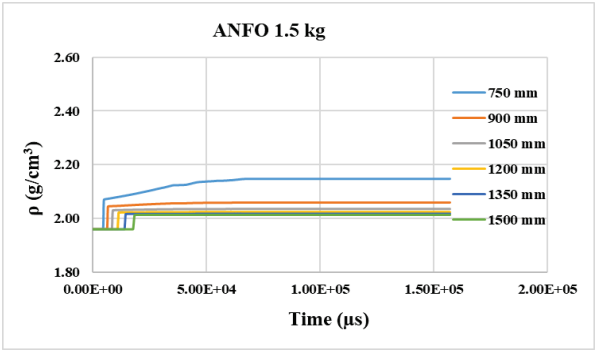

Fig. 9. Density profile of surrounding soil (1.5 kg of ANFO).

By analyzing the data, it was observed that for different charge masses of the same explosive, the zones remain the same with minimal density deviations, except for the mass of 1.5 kg. The dependence of the density of the soil after detonation on the mass of the explosive charge is shown in the graph in Figure 10.

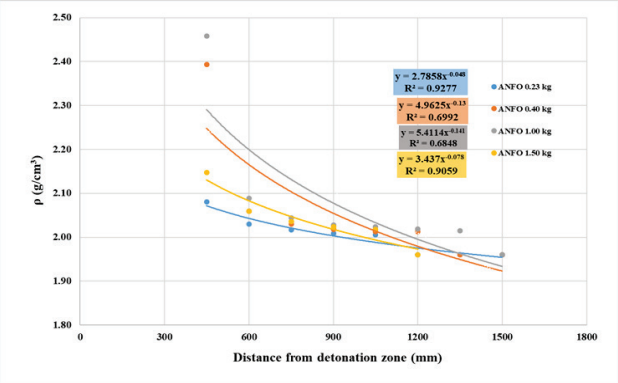

Fig. 10. The dependence of the density of the soil after detonation on the mass of the explosive charge.

The graphs show relatively strong correlations and the patterns are applicable for estimating the soil density in the vicinity of the resulting expansion.

At a mass of 1.5 kg, a change in zones occurs, i.e. at this mass of explosive, a larger expansion radius occurs and thus zones I and II disappear. Given the observations, an analysis of the dependence of the explosive mass on the expansion radius was conducted. The analysis is graphically presented in Figure 11.

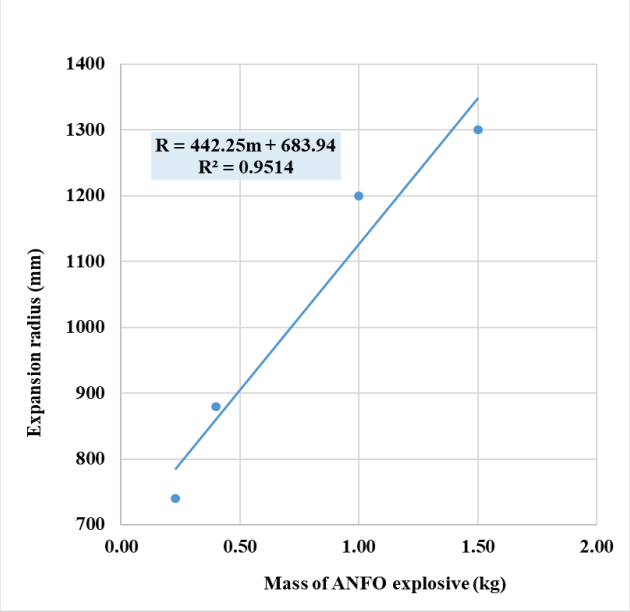

Fig. 11. Dependence of the radius of expansion in relation to the applied mass of explosives.

By analyzing the dependence of the radius of expansion in relation to the applied mass of explosives, a strong relationship was observed, and it can be assumed that by applying the expression:

$$R = 442.25m + 683.94 \quad (4)$$

It can estimate the radius of expansion of coherent soil when ANFO explosive is applied.

4. Conclusion

According to the conducted modeling and analysis and comparison with experimental data, it can be concluded that the radius of expansion does not depend significantly on the type of commercial explosive, that is, the product of the theoretical detonation energy with the volume of the resulting gaseous products is relevant.

From this fact, a connection can be drawn to the overall effect of the detonation effect, which is not necessarily only the effect of the shock wave on the detonation front, but is the sum of the effects of the subsequent expansion of gases.

Using the applied model, the geometric characteristics of the resulting expansion can be estimated with sufficient accuracy for engineering purposes for the soil conditions and the explosive used. In doing so, special attention should be paid to the parameters of the non-ideal detonation explosive with which the simulation is entered, as well as to the input parameters related to the characteristics of the soil for which the modeling is carried out.

5. References

[1] Wang, Z.; Hao, H.; Lu, Y. A three-phase soil model for simulating stress wave propagation due to blast loading. Int. J. Numer. Anal. Methods Geomech. 2004, 28, 33–56.

[2] Wang, Z.; Lu, Y. Numerical analysis on dynamic deformation mechanism of soil under blast loading. Soil Dyn. Earthq. Eng. 2003, 23, 705–714.

[3] Henrych, J. The Dynamics of Explosion and Its Use, 1st ed.; Elsevier Scientific Publishing Company: Amsterdam, The Netherlands, 1979; pp. 259–269.

[4] Fickett,W.; Davis,W.C. Detonation: Theory and Experiment; reprint; Dover Publications Inc.: New York, NY, USA, 2000; p. 386.

[5] Cooper, P.W. Explosives Engineering, 1st ed; Wiley-VCH:Weinheim, Germany, 2018; p. 480.

[6] Zukas, J.A.; Walters, W.P. Explosive Effect and Applications, 1st ed.; Springer Science & Business Media: New York, NY, USA, 1998; p. 433.

[7] Dobrilovic, M.; Dobrilovic, I.; Suceska, M.; Težak, D. Numerical Simulation Study of Cavity Formation in Soil under Blast Load. Appl. Sci.2024, 14, 6790. https://doi.org/10.3390/app14156790

[8] ANSYS Autodyn, version 13.0; User′ s Manual Release 2010; ANSYSInc.: Canonsburg, PA, USA, 2010.

55th Ordinary Annual Assembly of the Croatian Academy of Engineering and the 3rd Mini Scientific and Professional Conference

On June 2, 2025, the 55th Ordinary Annual Assembly of the Croatian Academy of Engineering (HATZ) was held in the Great Lecture Hall of the Faculty of Architecture, Faculty of Geodesy and Faculty of Civil Engineering of the University of Zagreb.

The Assembly was divided into two parts: a working part and a ceremonial part. During the working part, the members were informed about the financial situation of the Academy, the work of the Governing Board, the Departments, the Committees, the Centre, the Enterpreneurial and Scientific Councils, and on the Academy's publishing activities. At the same time, the new edition of the Yearbook for 2024 was presented, which contains ten scientific, technical and review papers by Academy members on the topic of the energy transition and the CAETS reporton the energy transition in the transport sector. In the ceremonial part of the Assembly, diplomas were awarded to new associate members, full members, emeritus members, international members and supporting members, as well as awards to the winners of the Academy Awards for 2024.

The Assembly was attended by members of the Academy and distinguished guests from academia and industry. The Assembly was welcomed by Prof. Mladen Zrinjski, PhD, Dean of the Faculty of Geodesy of the University of Zagreb, and Mr Luka Juroš, Head of the City of Zagreb's Department of Education, Sports and Youth.

The status of a new emeritus member of HATZ was acquired by Prof. Emeritus Ivica Grbac, PhD from the Department of Bioprocess Engineering.

At the meeting, the diplomas were awarded to the emeritus members who had acquired their status at the 53rd (electronic) Assembly held on February 11-13, 2025:

- Academician Mladen Obad Šćitaroci and Prof. Emeritus Tihomir Jukić, PhD, Department of Architecture and Urban Planning,
- Prof. Darovan Tušek, PhD, Department of Architecture and Urban Planning,
- Prof. Emeritus Frano Barbir, PhD, Prof. Nikola Čavlina, PhD and Prof. Nenad Debrecin, PhD, Department of Power Systems,
- Prof. Mirta Baranović, PhD, Department of Information Systems,
- Prof. Željko Domazet, PhD, and Academician Jurica Sorić, Department of Mechanical Engineering and Naval Architecture,
- Prof. Željko Hocenski, PhD, Department of Systems and Cybernetics.

The following full members were appointed:

- Prof. Mladen Zrinjski, PhD, Department of Civil Engineering and Geodesy,
- Prof. Antonio Šarolić, PhD, Department of Communication Systems,
- Prof. Zdenka Zovko Brodarac, PhD, Deppartment of Mining and Metallurgy,
- Prof. Stjepan Bogdan, PhD, Department of Systems and Cybernetics.

Following new associate members were appointed:

- Assoc. Prof. Željka Jurković, PhD, Department of Architecture and Urban Planning,
- Prof. Jasna Novak, PhD and Assoc. Prof. Vjekoslav Živković, PhD, Department of Bioprocess Engineering,
- Assoc. Prof. Marinko Kovačić, PhD and Prof. Jonatan Lerga, PhD, Department of Electrical Engineering and Electronics,
- Assoc. Prof. Tomislav Pukšec, PhD and Prof. Daniel Rolph Schneider, PhD, Department of Power Systems,
- Assoc. Prof. Alan Jović, PhD and Prof. Lea Skorin-Kapov, PhD, Department of Information Systems,
- Prof. Ljudevit Krpan, PhD, Department of Transport,
- Prof. Natalija Dolić, PhD and Prof. Borivoje Pašić, PhD, Department of Mining and Metallurgy,
- Assoc. Prof. Neven Alujević, PhD and Assoc. Prof. Milan Vujanović, PhD, Department of Mechanical Engineering and Naval Architecture,
- Prof. Hrvoje Džapo, PhD, Prof. Damir Seršić, PhD and Prof. Mario Vašak, PhD, Department of Systems and Cybernetics,
- Prof. Anica Hursa Šajatović, PhD, Department of Textile Technology.

New international members have been admitted to the HATZ:

- Prof. Georgia Butina Watson, PhD, Department of Architecture and Urban Planning,
- Prof. Emeritus Midhat Jašić, PhD, Department of Bioprocess Engineering.

The Croatian Academy of Engineering Awards for the year 2024 were awarded at the Assembly.

The annual "Rikard Podhorsky" award went to Prof. Meho Saša Kovačević, PhD, from the Department of Civil Engineering and Geodesy, and the "Vera Johanides" award for young scientists (for science) went to Tomislav Baškarad, PhD, from the University of Zagreb, Faculty of Electrical Engineering and Computing, Assoc. Prof. Tin Benšić, PhD, from the J. J. Strossmayer University of Osijek, Faculty of Electrical Engineering, Computer Science and Information Technology, and Ivana Čorak, PhD, from the University of Zagreb, Faculty of Textile Technology. The sponsor of the awards was the company CENTAR ZA VOZILA HRVATSKE d. d.

Immediately before the 55th Assembly, the 3rd Mini Scientific and Professional Conference "Croatian Academy of Engineering – a cohesive factor of engineering and biotechnical sciences and the Croatian economy" was held. The lectures were given by the winners of the "Vera Johanides" award, which the Croatian Academy of Engineering awards annually for the year 2024. Tomislav Baškarad, PhD gave a lecture entitled "The influence of renewable energy sources on the frequency regulation of the power system", Assoc. Prof. Tin Benšić, PhD gave a lecture entitled "Co-simulations and real-time simulations as a prerequisite for digital twins", and Ivana Čaorak, PhD, gave a lecture entitled "Bio-innovated polyester material for targeted use in the hospital environment".

The Assembly, was followed by an academic gathering held under the auspices of the SDEWES Center.

Engineering Power – *Bulletin of the Croatian Academy of Engineering*
Publisher: Croatian Academy of Engineering (HATZ), 28 Kačić Street,
P.O. Box 14, HR-10000 Zagreb, Republic of Croatia
Editor-in-Chief: Prof. Vedran Mornar, Ph.D., President of the Academy, University of Zagreb, Faculty of Electrical Engineering and Computing
Editor: Prof. Bruno Zelić, Ph.D., Vice-President of the Academy, University of Zagreb, Faculty of Chemical Engineering and Technology
Guest Editor: Prof. Mario Dobrilović, Ph.D., University of Zagreb, Faculty of Mining, Geology and Petroleum Engineering
Activities Editor: Tanja Miškić Rogić
Editorial Board: Prof. Vedran Mornar, Ph.D., Prof. Vladimir Andročec, Ph.D., Prof. Bruno Zelić, Ph.D., Assoc. Prof. Mario Bačić, Ph.D., Prof. Neven Duić, Ph.D.
Editorial Board Address: Croatian Academy of Engineering (HATZ), "Engineering Power" – Bulletin of the Croatian Academy of Engineering, Editorial Board, 28 Kačić Street, P.O. Box 14, HR-10000 Zagreb, Republic of Croatia
E-mail: hatz@hatz.hr
Graphical and Technical Editor: Grafika Gracer d.o.o., Celje

Vol. 20(1) 2025 – ISSN 2718-322X (Online)